Molecular Microbiology (2019) 0(0), 1–20 doi:10.1111/mmi.14185

Inhibition of *Pseudomonas aeruginosa* and *Mycobacterium tuberculosis* disulfide bond forming enzymes

Cristina Landeta,[1] Laura McPartland,[1] Ngoc Q. Tran,[1] Brian M. Meehan,[1] Yifan Zhang,[1] Zaidi Tanweer,[2] Shoko Wakabayashi,[3] Jeremy Rock,[3] Taehyun Kim,[1] Deepak Balasubramanian,[1] Rebecca Audette,[3] Melody Toosky,[3] Jessica Pinkham,[3] Eric J. Rubin,[3] Stephen Lory,[1] Gerald Pier,[2] Dana Boyd[1] and Jon Beckwith[1]*

[1] *Department of Microbiology and Immunobiology, Harvard Medical School, Boston, MA, USA.*

[2] *Division of Infectious Diseases. Department of Medicine. Brigham and Women's Hospital, Harvard Medical School, Boston, MA, USA.*

[3] *Department of Immunology and Infectious Diseases, Harvard School of Public Health, Boston, MA, USA.*

Summary

In bacteria, disulfide bonds confer stability on many proteins exported to the cell envelope or beyond, including bacterial virulence factors. Thus, proteins involved in disulfide bond formation represent good targets for the development of inhibitors that can act as antibiotics or anti-virulence agents, resulting in the simultaneous inactivation of several types of virulence factors. Here, we present evidence that the disulfide bond forming enzymes, DsbB and VKOR, are required for *Pseudomonas aeruginosa* pathogenicity and *Mycobacterium tuberculosis* survival respectively. We also report the results of a HTS of 216,767 compounds tested against *P. aeruginosa* DsbB1 and *M. tuberculosis* VKOR using *Escherichia coli* cells. Since both *P. aeruginosa* DsbB1 and *M. tuberculosis* VKOR complement an *E. colidsbB* knockout, we screened simultaneously for inhibitors of each complemented *E. coli* strain expressing a disulfide-bond sensitive β-galactosidase reported previously. The properties of several inhibitors obtained from these screens suggest they are a starting point for chemical modifications with potential for future antibacterial development.

Accepted 6 December, 2018. *For correspondence. E-mail jon_beckwith@hms.harvard.edu.

© 2018 John Wiley & Sons Ltd

Abbreviations: β-Gal^{dbs}, Disulfide-bond sensitive β-Galactosidase (MalF-LacZ102). LacZ fused to the membrane protein MalF, localizes LacZ in the periplasm making it sensitive to disulfide bond formation; X-Gal, 5-Bromo-4-chloro-3-indolyl galactopyranoside; CFU, Colony forming units; IPTG, Isopropyl β-D-1-thiogalactopyranoside; MIC, Minimal Inhibitory Concentration; MBC, Minimal Blue Concentration, the minimal concentration required to see a pale blue color indicating inhibition of DsbB or VKOR in *E. coli* cells expressing β-Gal^{dbs}; HTS, High Throughput Screening; NEM, N-Ethylmaleimide; Mal-PEG, α-[3-(3-Maleimido-1-oxopropyl)amino]propyl-ω-methoxy, polyoxyethylene; ATc, Anhydrotetracycline; SAR, Structure-activity relationship; PDI, Protein disulfide isomerase.

Introduction

Disulfide bonds confer activity to many proteins by stabilizing them in their active conformations. The formation of disulfide bonds in proteins is an oxidative process that generates a covalent bond linking the sulfur atoms of two cysteine residues. In bacteria, structural disulfide bonds are found in proteins of the cell envelope and they play a role in folding and stability of proteins involved in important cellular processes such as cell division, motility, virulence of pathogenic bacteria, transport of virulence proteins into the host cells, response to environmental threats and assembly of the outer membrane of Gram-negative bacteria (Landeta *et al.,* 2018).

The formation of disulfide bonds in *E. coli* utilizes the thioredoxin-family protein DsbA, which catalyzes through its CXXC active site the formation of sulfur-sulfur bonds between pairs of cysteines in substrate proteins (Bardwell *et al.,* 1991). In the process, DsbA becomes reduced thus necessitating a second enzyme DsbB to regenerate DsbA's activity by transferring DsbA's electrons to quinone (Bardwell *et al.,* 1993). While the DsbAB system is widespread in Gram-negative bacteria, Actinobacteria and Cyanobacteria use the protein VKOR (vitamin K epoxide reductase) instead of DsbB to

oxidize DsbA (Dutton *et al.,* 2008). Bacterial VKOR is a homolog of the vertebrate protein VKOR, an endoplasmic reticular enzyme which maintains the reduced form of vitamin K, a cofactor in the post-translational modification of proteins involved in blood coagulation (Kurosu and Begari, 2010). Bacterial VKOR is the target of the anticoagulant drug warfarin (Dutton *et al.,* 2010). DsbB and VKOR share no protein sequence homology but they exhibit similar structural features and contain a quinone cofactor to generate a disulfide bond *de novo* (Inaba *et al.,* 2009; Li *et al.,* 2010). In fact, the interactions between the redox-active cysteines of DsbA and VKOR proceed by the same steps seen between DsbA and DsbB (Wang *et al.,* 2011). Furthermore, VKORs from other bacteria and one eukaryote can complement an *E. coli* with a *dsbB* deletion (Dutton *et al.,* 2008; Hatahet *et al.,* 2015).

Given that disulfide bond formation contributes to the pathogenicity of bacteria, proteins involved in disulfide bond formation represent good targets for the development of inhibitors that can act as antibiotics or anti-virulence agents, since inhibition of this process would result in the simultaneous inactivation of several types of virulence factors. We have previously reported that a highly sensitive assay for detecting defects in disulfide bond formation allows the identification of compounds potentially useful in the development of antibiotics (Landeta *et al.,* 2015). This assay detects inhibition of disulfide bond forming enzymes in growing *E. coli* cells using a version of *E. coli* β-Galactosidase (β-Gal^{dbs}) that is only active when the functionality of the disulfide bond formation pathway is inactivated. The screening of compounds is performed in parallel for inhibition of the non-homologous enzymes, DsbB and VKOR from another bacteria (Fig. 1). This approach allows us to search for inhibitors for one or the other protein. The parallel screening thus provides reciprocal controls that eliminate inhibitors that are influencing β-galactosidase activity by acting directly on DsbA or affecting membrane protein assembly, since those molecules would appear as hits in screens for both proteins. Specific inhibitors would only register as hits against one strain or the other (Landeta *et al.,* 2015). While it is formally possible that a particular compound could inhibit both DsbB and VKOR, the sequence dissimilarity between the two would make it unlikely.

Using this methodology in a previous screen of 50,000 molecules, we found a family of compounds structurally related to pyridazinones that inhibit DsbB enzymes from several Gram-negative pathogenic bacteria (Landeta *et al.,* 2015). Structure-activity relationship (SAR) analyses yielded more effective DsbB pyridazinone-related inhibitors, such as compounds 12 and 36 (Landeta *et al.,* 2015; 2017) (Fig. 3). This class of drugs inhibits DsbB by binding covalently to the second cysteine of DsbB (Cys44) thus preventing the recycling of DsbB by quinones (Landeta *et al.,* 2015; 2017). These molecules do not inhibit cysteine-containing enzymes such as DsbA, human protein disulfide isomerase (PDI) or VKOR, but they do react with reduced glutathione, which can potentially lead to unfavorable toxicological outcomes (Potashman and Duggan, 2009).

In this work, we focused on two important human pathogens, namely *Pseudomonas aeruginosa* and *Mycobacterium tuberculosis*. *P. aeruginosa* is one of the six pathogens for which new antibacterial agents are most desperately needed (Rice, 2010). It is a Gram-negative organism often associated with extremely difficult-to-treat infections that resist antibiotic treatments and can cause a variety of infections in a wide range of tissue types where mortality rates of more than 60% have been reported (Page and Heim, 2009). Infections include acute pneumonia, ulcerative keratitis, bacteremia, urinary tract, intra-abdominal, chronic airway and wound infections (Lyczak *et al.,* 2000; Page and Heim, 2009). This organism frequently emerges as a threat to neutropenic, immunosuppressed patients undergoing treatment for cancer wherein the spread of antibiotic-resistant organisms from gastrointestinal sites into the blood stream or in the setting of cystic fibrosis has also been observed (Maschmeyer and Braveny, 2000; Fujitani *et al.,* 2011; Folkesson *et al.,* 2012). *P. aeruginosa* harbors two *dsbA* and two *dsbB* homologs. Disulfide bond formation is mainly driven by DsbA1 which is reoxidized by both DsbB1 and DsbB2 (Ha *et al.,* 2003; Arts *et al.,* 2013), while DsbA2 is unable to complement *dsbA1* mutant and its function remains unknown (Arts *et al.,* 2013) (See Results). Some *Pseudomonas* virulence factors known to contain disulfide bonds are the assembly of pilin protein (PilA) involved in twitching motility (Ha *et al.,* 2003; Harvey *et al.,* 2009), the elastolytic metalloprotease, elastase (LasB) and exotoxin A (Madshus and Collier, 1989; Braun *et al.,* 2001; Urban *et al.,* 2001). Furthermore, for certain virulence factors, the disulfide bond formation pathway is required for their proper secretion, including the two type-III effectors ExoT and ExoU (Ha *et al.,* 2003) as well as other exoproteins such as the chitin-binding protein (CbpD), an immunomodulating metalloprotease IMPa and proteases PaAP and PrpL (Arts *et al.,* 2013). In addition, the *P.aeruginosadsbA1* mutant was detected in a screen for virulence factors in a *D. melanogaster* infection model, and was confirmed to be avirulent in a peritoneal mouse infection model (Kim *et al.,* 2008). We hypothesized that the failure to find DsbB mutants in such a screen was due to the redundancy of DsbB. On the contrary, *M. tuberculosis* is a Gram-positive organism that causes tuberculosis, one of the leading causes of infectious disease deaths worldwide (World Health Organization, 2017). The pathway that introduces disulfide bonds into proteins in *M. tuberculosis* utilizes a VKOR instead of DsbB to oxidize mycobacterial DsbA (Dutton *et al.,* 2008;

Ke *et al.,* 2018). The mechanism of electron transfer between DsbA, VKOR and quinones is analogous to that observed between DsbA, DsbB and quinones (Dutton *et al.,* 2008; Wang *et al.,* 2011; Ke *et al.,* 2018). Additionally, VKOR has been shown to be essential for growth of *M. tuberculosis* and *M. smegmatis* (Sassetti and Rubin, 2003; Dutton *et al.,* 2010), likely because one or more essential proteins require disulfide bonds to be active.

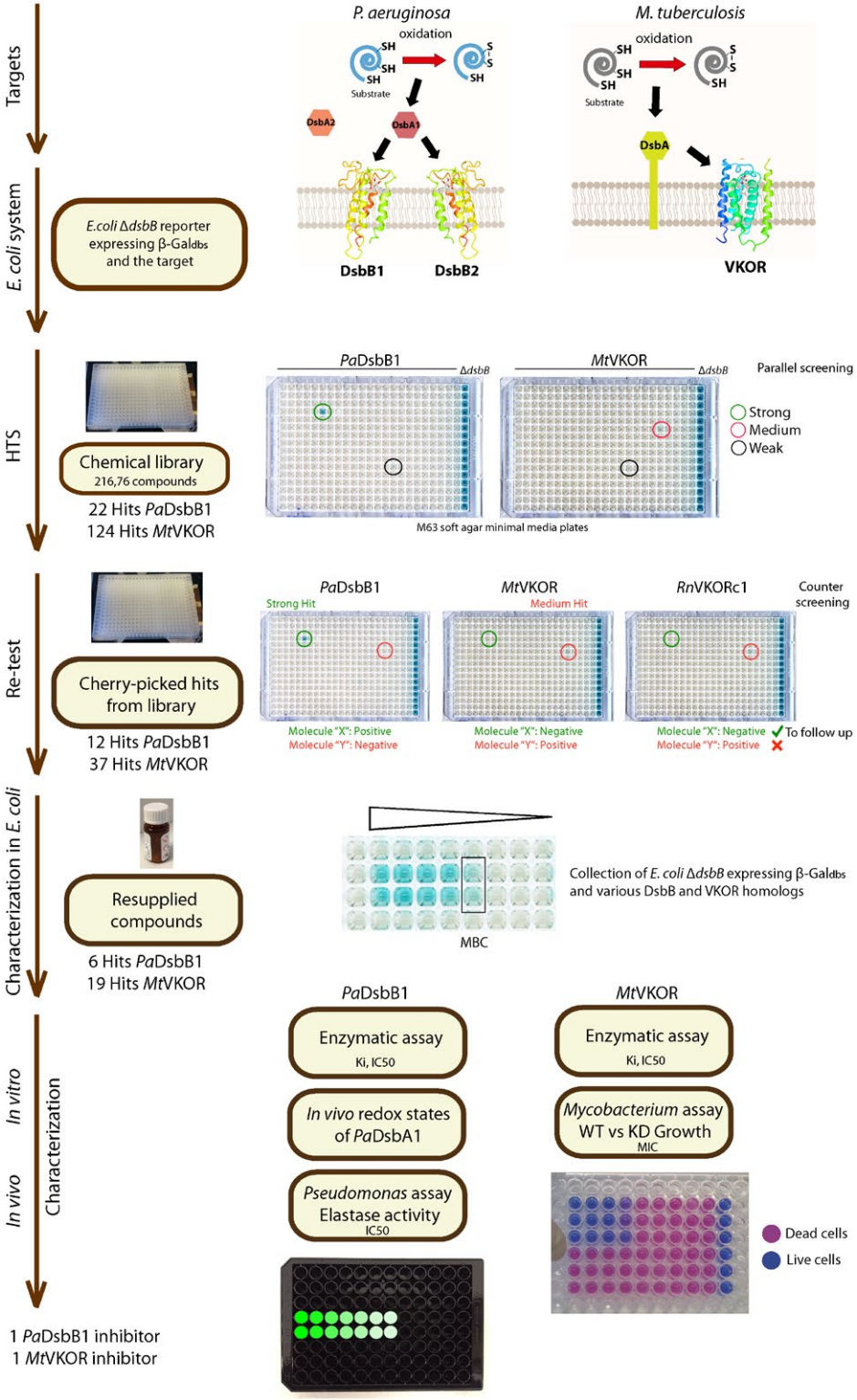

Fig. 1. Outline of screening and inhibitor selection. The first step 'Targets' represents the disulfide bond forming systems of two human pathogens, *P. aeruginosa* and *M. tuberculosis*. The second step '*E. coli* system' indicates the expression of the targets, *Pa*DsbB1 (CL523 strain) and *Mt*VKOR (CL382 strain), in *E. coli* reporter strain expressing β-Gal^{dbs}. The third step 'HTS' indicates the high throughput screening of 216,767 compounds and shows an example of strong, medium and weak hits on agar minimal media plates. In the fourth step 'Re-test', the compounds were cherry picked from the chemical library and tested against the strains used in screening plus two additional *E. coli* counter-screening strains expressing low levels of *Ec*DsbB and *Mt*VKOR (DHB7935 and DHB7657 strains respectively) and one additional strain expressing *Rn*VKOR (FSH250 strain) to discard molecules with unwanted anticoagulant side effect. The next step 'Characterization in *E. coli*' involved resupplying the molecules selected in the previous stage, making serial dilutions on agar plates and testing them against a collection of *E. coli* strains expressing VKOR proteins and various DsbB proteins from Gram-negative pathogens in order to determine their MBCs (minimal concentration of give a pale blue color indicating inhibition of DsbB or VKOR in *E. coli* cells expressing β-Gal^{dbs}). Finally, '*In vivo* and *in vitro* characterization' involved determination of Ki and IC50 for all compounds in a ubiquinone reduction assay with purified enzymes. For *Pseudomonas* inhibitors, the *in vivo* redox states of *Pa*DsbA1 (the substrate of the two *Pa*DsbB proteins) was also determined in the presence of compound as well as the activity of elastase (a substrate of *Pa*DsbA1) using a fluorescent assay. On the contrast, *Mycobacterium* inhibitors were tested in a growth assay using wild type and a *vkor* knockdown (KD) strain. See text for further details.

In contrast, the Dsb pathway in *E. coli* is only essential under anaerobic growth (Meehan *et al.*, 2017a).

Thus, here we sought to determine the impact of disulfide bond formation in the virulence of *P. aeruginosadsb* mutants and the redundancy in the Dsb system using lung and corneal infections in murine model, two models that best mimic *P. aeruginosa* human infections (Preston *et al.,* 1995; Mizgerd and Skerrett, 2008; Zhao *et al.,* 2016). We also constructed a conditionally lethal strain of *M. tuberculosis* using a tunable CRISPR interference platform (Rock *et al.,* 2017) to knock down *vkor* and used it as a tool to determine VKOR inhibition in *M. tuberculosis*. We then performed a High Throughput Screen (HTS) of 216,767 compounds tested against the *P. aeruginosa* DsbB1 (*Pa*DsbB1) and *M. tuberculosis* VKOR (*Mt*VKOR) enzymes using *E. coli* cells expressing β-Gal^{dbs} in order to find inhibitors for antibacterial development against these two human pathogens. The properties of several inhibitors obtained from these screens suggest they are candidates with potential for future antibacterial development and a starting point for chemical modifications in order to improve their potency.

Results

P. aeruginosa strains defective in disulfide bond formation display attenuated virulence in lung and corneal infections

In order to determine the effect of disulfide bond formation in *P. aeruginosa* virulence we constructed the clean deletions of *dsbA1*, *dsbA2*, *dsbB1* and *dsbB2* genes as well as the double deletions of *dsbA1* and *dsbA2* (Δ*dsbA1A2*) and of *dsbB1* and *dsbB2* (Δ*dsbB1B2*) in *P. aeruginosa* UCBP-PA14 strain. Before assessing virulence *in vivo*, we tested two virulence-related phenotypes that *dsb* mutants display, namely the lack of twitching motility and elastase production (Urban *et al.,* 2001; Ha *et al.,* 2003; Arts *et al.,* 2013). Similar to previous results (Arts *et al.,* 2013), the Δ*dsbA1* as well as the Δ*dsbB1B2* mutant are unable to produce elastase (Fig. 2A) or twitch (Supplementary Fig. 1). We also determined complementation of the mutant strains by expressing the *dsb* genes from a plasmid. To this end, we cloned each of the four *dsb* genes in a plasmid (pJN105) under the control of their own promoters except for *dsbA2*, for which we used *dsbA1*'s promoter since it is unclear what conditions allow for expression of this gene (Arts *et al.,* 2013). We transformed these plasmids into the double deletion mutants and tested complementation of the resulting strains by looking at twitching motility and elastase production. Both *dsbB1* and *dsbB2* complemented motility and elastase of the Δ*dsbB1B2* mutant, consistent with previous reports (Arts *et al.,* 2013). However, only *dsbA1* but not *dsbA2* complemented the Δ*dsbA1A2* mutant (Data not shown).

We then used two murine models to test the virulence of *dsb* mutants, keratitis and pneumonia models. First, using a keratitis model we tested the virulence of the double *dsb* mutants and two of these complemented counterparts in C57BL/6 mice. We tested the two double knockouts of Δ*dsbA1A2* and Δ*dsbB1B2* in corneal infection by scratching the eyes with 10^7 CFU as reported previously (Preston *et al.,* 1995). We then scored the eye pathology (Fig. 2B, left) and determined the extracellular (Fig. 2B, center) and intracellular bacterial counts (Fig. 2B, right) of the corneas. Our results show that infection with Δ*dsbB1B2* mutant displayed a 60% reduction in the pathology score ($p < 0.05$), while Δ*dsbA1A2* mutant showed 87% reduction ($p < 0.001$). Additionally, the Δ*dsbB1B2* mutant has a 99 and 98% reduction in extracellular and intracellular bacterial counts, respectively, when compared to wild type ($p < 0.0001$). While the Δ*dsbA1A2* mutant yielded no bacteria in both cases ($p < 0.0001$).

We then determined the effect on virulence using two of the complemented strains in the keratitis model, the Δ*dsbA1A2* strain complemented with pJN105-*dsbA1* and the Δ*dsbB1B2* strain complemented with pJN105-*dsbB1* (Fig. 2C). The plasmids expressing *dsbA1* and *dsbB1* genes from a plasmid restored the virulence to the Δ*dsbA1A2* and Δ*dsbB1B2* mutants, respectively, as

observed by the higher eye pathology scores (Fig. 2C, left) or extracellular and intracellular bacterial counts (Fig. 2C, center and right). Thus, Δ*dsbA1A2* and Δ*dsbB1B2* mutants showed reduced virulence in the murine keratitis model and the virulence is restored when the mutants are complemented with the *dsbA1* or *dsbB1* genes respectively.

In addition to the keratitis model, we also determined the virulence of *dsb* mutants in a pneumonia model. We first conducted an experiment to determine the optimal bacterial density to infect the lungs of immunosuppressed ICR mice. We tested 10-fold dilutions ranging from 10^2 to 10^7 CFU/mouse of the *P. aeruginosa* wild-type strain and determined the bacterial counts in the lungs at 2 and 26 h after infection (Supplementary Fig. 2A and B and Supplementary Tables 2-1 to 2-6). We observed that 10^4 CFU/mouse resulted in an approximate 3-log increase in bacterial counts in a 24 h infection period and only

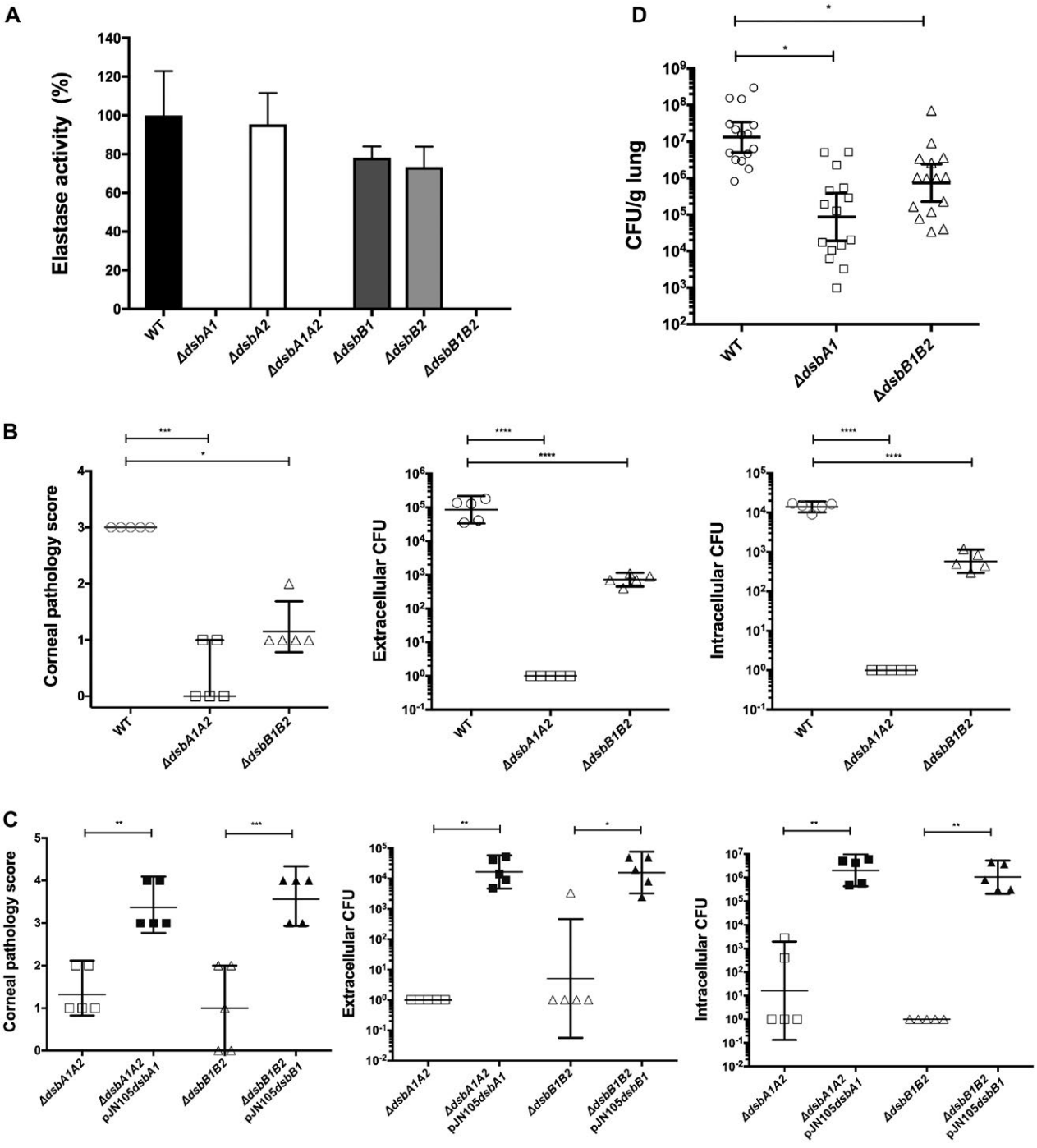

Fig. 2. Mutations in genes encoding disulfide bond forming enzymes in *P. aeruginosa* cause severe defects in virulence.
A. Δ*dsbA1* and Δ*dsbB1B2* mutants have little or no elastase activity (<0.1 μg mL^{-1} A_{600}^{-1}). Activity was measured in the supernatant of cell cultures grown in 96-well plates for 15 h at 37°C in M63 minimal medium supplemented with 0.2% glucose and 0.2% casamino acids. Values represent the average ±SD of at least three independent experiments.
B. Comparison of growth in corneal tissue between *P. aeruginosa* PA14 (CL418), Δ*dsbA1A2* (CL541) and Δ*dsbB1B2* (CL356) strains using C57BL/6 female mice. Groups of five mice were scratch-injured in the eyes and challenged with 5 μL of *P. aeruginosa* strains (~10^7 CFU/eye). The severity of corneal disease was scored by a masked observer after 48 h on a scale of 0 to 4: 0, eye macroscopically identical with the uninfected contralateral control eye; 1, faint opacity partially covering the pupil; 2, dense opacity covering the pupil; 3, dense opacity covering the entire anterior segment; 4, perforation of the cornea, phthisis bulbi (shrinkage of the globe after inflammatory disease), or both. Mice were euthanized and the corneas excised to determine extracellular and internalized *P. aeruginosa* CFU. Significance between mutants vs wild-type strain was determined by Kruskal Wallis test for pathology score and one-way ANOVA followed by Dunnett's test for CFU counts. Data represent individual values with the geometric mean and 95% confidence intervals.
C. Comparison of growth in corneal tissue between *P. aeruginosa* Δ*dsbA1A2* (CL541) and Δ*dsbB1B2* (CL356) mutants and these strains complemented with *dsbA1* or *dsbB1* genes expressed from a plasmid (pJN105). Groups of mice were treated as described in B. Significance between mutant vs complemented strain was determined by Kruskal Wallis test for pathology score and one-way ANOVA followed by Dunnett's test for CFU counts. Data represent individual values with the geometric mean and 95% confidence intervals.
D. Comparison of growth in lung tissue between *P. aeruginosa* PA14 (CL418), Δ*dsbA1* (CL384) and Δ*dsbB1B2* (CL356) strains using neutropenic ICR mice. Groups of 20 animals were rendered immune suppressed by two intraperitoneal injections of cyclophosphamide and were challenged intranasally (0.02 mL/lung) with bacteria (~10^4 CFU/mouse). Groups of five animals were sacrificed at 2 h after inoculation (Supplementary Fig. 2E), the rest (15 animals) were sacrificed at 26 h after inoculation and the lung tissues were harvested to enumerate bacteria. Significant difference ($p < 0.05$) compared to the parental strain was determined by one-way ANOVA followed by Dunnett's test. Data represent individual values with the geometric mean and 95% confidence intervals. *$p < 0.05$; **$p < 0.01$; ***$p < 0.001$; ****$p < 0.0001$.

one of six mice died at 26 h. Higher inoculum densities resulted in over 50% mortality at 26 h and lowering the inoculum yielded insufficient bacterial growth in lung tissues. Therefore, we used 10^4 CFU/mouse to evaluate the virulence of *dsb* mutants and increased the population size to 20 animals, from which 5 were sacrificed at 2 h and 15 were sacrificed at 26 h after infection (Fig. 2D, Supplementary Fig. 2E and Tables 4-1 to 4-5). We only used in this model the double Δ*dsbB1B2* and the single Δ*dsbA1* mutant given that *dsbA2* gene did not complement two phenotypes when expressed from a *dsbA1* promoter. Our results show that infection with Δ*dsbB1B2* double mutant yielded an 87% reduction in bacterial counts in lung tissue compared to wild type ($p < 0.05$, Fig. 2D), while Δ*dsbA1* yielded 98% reduction in bacterial counts compared to wild type ($p < 0.05$, Fig. 2D) at 26 h after infection. Therefore, both Δ*dsbA1* and Δ*dsbB1B2* mutants displayed attenuated virulence in the murine pneumonia model.

We also attempted to determine the virulence of *dsb* mutants using immune competent ICR mice, however this was not feasible due to poor growth and excessive variability of the wild-type strain in the pneumonia model (Supplementary Fig. 2C-D and Tables 3-1 to 3-7).

High throughput screening to find inhibitors of PaDsbB1 and MtVKOR in E. coli

Given the importance of DsbB proteins in the virulence of *P. aeruginosa* (above) and of VKOR in the growth of *M. tuberculosis* (Sassetti and Rubin, 2003; Dutton *et al.,* 2010), we screened for inhibitors of both proteins simultaneously using an approach described previously (Landeta *et al.,* 2015). That the Δ*dsbA1* mutant displayed a slightly more severe virulence phenotype in *P. aeruginosa* than the DsbB double mutant might suggest that DsbA1 would also be a useful target. However, DsbA belongs to the widespread thioredoxin family and inhibitors of DsbA may also inhibit one of the many other thioredoxin family members that in humans contribute to the reducing environment of the cytoplasm and to protein folding in the endoplasmic reticulum. On the contrary, DsbB has no known homologs in eukaryotes, thus making it more suitable for developing virulence inhibitors. Being that DsbB and VKOR do not share protein sequence homology they can be used to counter screen molecules in order to find more specific inhibitors for each. Since both the *P. aeruginosa* DsbB homologs and the *M. tuberculosis* VKOR complement *E. coli dsbB* null mutants, we can screen simultaneously for inhibitors of each complemented strain in 384-well plates seeking compounds that inhibit one protein but not the other. Inhibition is scored visually through the appearance of blue color in a well due to increased activity of the disulfide-bond sensitive β-galactosidase (β-Gal^{dbs}) (Fig. 1) (Landeta *et al.,* 2015). In these strains, strong inhibition of disulfide bond formation should lead to a substantial increase in β-galactosidase activity (Bardwell *et al.,* 1991; Tian *et al.,* 2000). For the screening of *Pseudomonas* DsbB, we expressed the DsbB1 homolog in *E. coli* from an IPTG-inducible promoter in a pDSW206 plasmid (CL523 strain). For the *Mycobacterial* VKOR screen, we expressed the *vkor* gene in *E. coli* from a strong IPTG-inducible promoter in a pTrc99a plasmid (CL382 strain). Our previous screening strain expressed *vkor* from an IPTG-inducible promoter in the chromosome and this strain did show a very pale blue color, indicating that the *Mt*VKOR did not completely restore levels of disulfide bond formation in the *E. coli dsbB* deletion (Dutton *et al.,* 2010). The higher copy number of the plasmid led to better complementation of the re-oxidation of *Ec*DsbA (Supplementary Fig. 3) and hence to lower β-galactosidase background.

We carried out a HTS of 216,767 compounds, tested in duplicate, against the *P. aeruginosa* DsbB1 (*Pa*DsbB1) and *M. tuberculosis* VKOR (*Mt*VKOR) enzymes using *E. coli* cells (Fig. 1). The libraries were part of the collection of the Institute of Chemistry and Cell Biology (ICCB) at Harvard Medical School (Supplementary Table 1A). In addition to the *E. coli* Δ*dsbB* strain as negative control, we used two molecules as positive and negative controls for each strain that were placed in column 2 of agar plates. One is the anticoagulant bromindione, which inhibits *Mt*VKOR as well as human VKOR but not *Pa*DsbB1 and the other molecule is compound 12 a dichloropyridazinone, which inhibits *Pa*DsbB1 but not *Mt*VKOR (Fig. 3 and Supplementary Fig. 4) (Landeta *et al.,* 2015). The hits found in HTS were classified by the intensity of the blue signal on agar plates, as strong, medium, weak or very weak (Fig. 1) (Landeta *et al.,* 2015). We found 22 hits of *Pa*DsbB1 and 124 hits of *Mt*VKOR that appeared in both replica plates from the 216,767 compounds tested (Supplementary Table 1B). Testing the effects of compounds on the two strains in parallel allowed us to pick candidate inhibitors that are specific to either *Pa*DsbB1 or *Mt*VKOR. Therefore, we eliminated from further consideration compounds giving positive signals with both strains since these are most likely inhibiting *Ec*DsbA or less likely cytoplasmic membrane protein assembly (Landeta *et al.,* 2015). From all the compounds tested, we only found 3 hits that inhibited both strains (Supplementary Fig. 5).

We re-tested all the hits against the two strains used for HTS as well as their respective counter-screening strains, i.e. strains that show a very pale blue background due to lower expression of either DsbB or VKOR (Fig. 1). These strains were used in order to detect weak inhibitors that are not specific to each strain, that is for *Pa*DsbB1 inhibitors, a strain expressing low levels of *Mt*VKOR (DHB7657 strain) while for *Mt*VKOR inhibitors, a strain expressing low levels of *Ec*DsbB (DHB7935 strain). Given the importance of the human VKOR homolog in the activation of blood clotting factors, we also screened hits with an additional *E. coli* mutant strain expressing a rat (*Rattus novergicus*) VKOR homolog (*Rn*VKOR, FSH250 strain) which conferred upon the strain the ability to oxidize *Ec*DsbA (Hatahet *et al.,* 2015). This was done in order to discard compounds that may have an unwanted anticoagulant side effect. We found 9 potential inhibitors of *Pa*DsbB1 that share similarity to pyridazinone molecules and had weaker activity than the compounds we found and studied previously (Landeta *et al.,* 2015; 2017). These were not re-tested. For the remaining compounds, the retest yielded a repeat rate of 92% (12/13) for *Pa*DsbB1 inhibitors and 30% (37/124) for *Mt*VKOR (Supplementary Table 1B). The low rate observed for *Mt*VKOR was due to the low repeat rate among weak and very weak hits (Supplementary Table 1B).

In the re-test, we also found that 4 *Pa*DsbB1 hits inhibited the counter-screening *Mt*VKOR strain (DHB7657

Table 1. Analysis of *Pa*DsbB1 inhibitors.

	Elastase *in vivo* assay IC_{50} (μM)[a]			*In vitro* assay[b]						
		*Pa*DsbB1	*Pa*DsbB2	*Pa*DsbB1		*Pa*DsbB2		*Ec*DsbB		PDI[c]
ID	WT	(Δ*dsbB2)*	(Δ*dsbB1*)	IC_{50} (μM)	Ki (μM)	IC_{50} (μM)	Ki (μM)	IC_{50} (μM)	Ki (μM)	IC_{50} (μM)
12	228.8 (170.6–306.8)	8.6 (5.48–13.63)	0.01 (0.006–0.02)	4.1 ± 0.6	3 ± 0.2	6 ± 1	4 ± 0.2	0.014 ± 0.0001	0.005 ± 0.001	N
36	89 (60.4–131.3)	2.2 (1.2–3.89)	0.025 (0.019–0.033)	4 ± 0.37	4 ± 0.4	3 ± 0.5	2.7 ± 0.1	0.01 ± 0.001	0.002 ± 0.0005	N
PA1	279.8 (96.8–808.3)	120.7 (83.7–173.9)	29.5 (23.6–36.9)	530 ± 60	ND	600 ± 50	ND	150 ± 50	100 ± 30	N
PA2	N	N	N	83 ± 17	ND	83 ± 13	ND	37.5 ± 5	30 ± 7	98.34 (65.45–147.8)
PA3	646.4 (436.7.7–956.9)	9 (5.5–14.83)	1.26 (0.64–2.47)	6 ± 0.6	2.8 ± 0.2	3 ± 0.11	7.5 ± 0.8	17 ± 2	13 ± 1.5	98.02 (45.03–213.4)
PA4	144.8 (103.1–203.5)	101.2 (86.04–119.1)	2.1 (1.6–2.8)	15 ± 1	17 ± 1.2	23 ± 5	16 ± 1.5	17 ± 1	10 ± 1.2	82.03 (35.99–186.9)
PA5	N	N	N	9 ± 1	4.25 ± 0.5	18 ± 3	9 ± 1.5	6 ± 0.5	6 ± 1	N
PA6	139.8 (92.1–212.2)	16.5 (12.5–21.8)	5 (4.2–6.03)	26 ± 3.5	12 ± 1.4	25 ± 4	18 ± 2	3 ± 0.1	5 ± 1	59.6 (31.55–112.6)

Abbreviations: ND, Not determined; N, No inhibition observed up to 100 μM.

Data represent the average of at least two independent experiments with 95% confidence intervals in parenthesis or ±SD.

[a]*In vivo* inhibition was determined as elastase activity in the supernatant of cell cultures after 15 h incubation at 37°C in M63 minimal medium supplemented with 0.2% glucose, 0.2% casamino acids and serial dilutions of drug dissolved in DMSO.

[b]*In vitro* inhibition was measured by following the reduction of ubiquinone with purified His-tagged enzymes. The assay used 10 nM of *Pa*DsbB1/*Pa*DsbB2 or *Ec*DsbB with 20 μM reduced-*Pa*DsbA1 or *Ec*DsbA and 25 μM Ubiquinone-1. For K_i determination 1-100 μM of Ubiquinone-1 was used.

[c]PDI activity was measured using the insulin reduction assay.

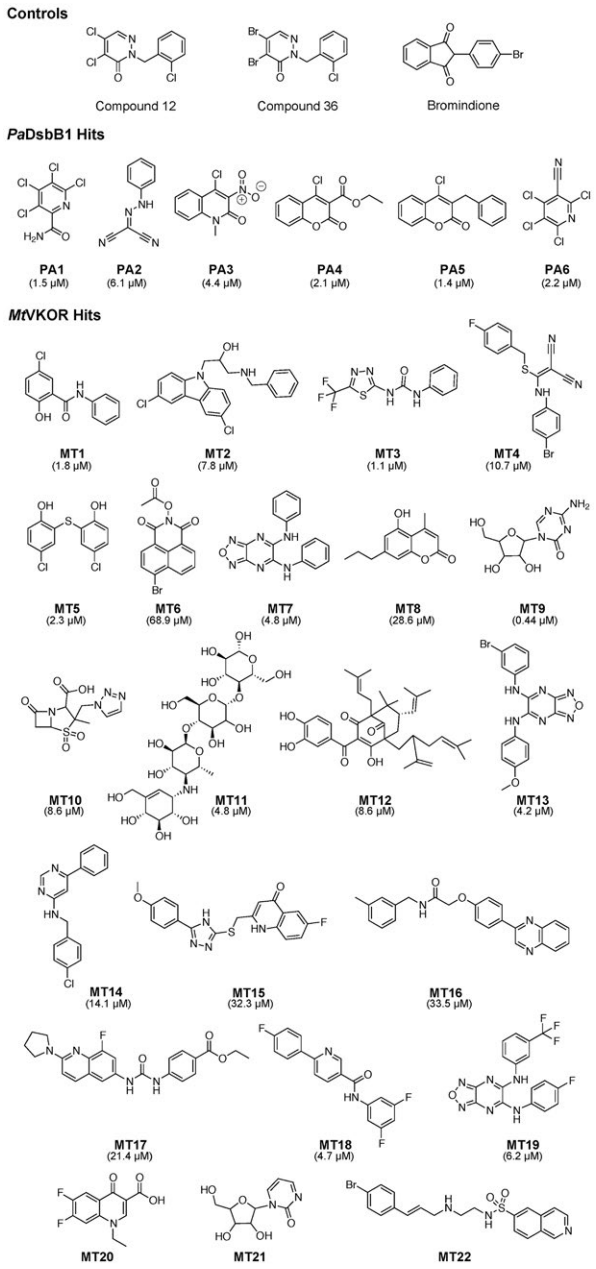

Fig. 3. Structures of inhibitors found in HTS. Control compounds include 12 and 36, which are inhibitors of DsbB enzymes, while Bromindione is a known anticoagulant that targets *Mt*VKOR and *Rn*VKOR enzymes. The structures of six *Pa*DsbB1 inhibitors and 22 *Mt*VKOR inhibitors found to inhibit the respective enzyme in the HTS using *E. coli* reporter strain (CL523 and CL382 respectively). The MBCs are reported below for each of the molecules except the last three molecules that were not resupplied from commercial libraries. The MBC is the minimal concentration required to produce a pale blue color in *E. coli* cells expressing β-Gal^{dbs} indicating inhibition of DsbB or VKOR. The results represent the average of at least two independent experiments.

strain) and 2 hits inhibited the *Rn*VKOR strain (FSH250 strain). Thus, from the 12 *Pa*DsbB1 hits that repeated only 6 hits were candidates to follow up. Among the 37 *Mt*VKOR hits that repeated, 5 of them had the same structure thus leaving only 33 unique hits. From these, 3 inhibited our counter-screening *Ec*DsbB strain (DHB7935 strain) and 8 inhibited the *Rn*VKOR strain, which left us with 22 candidates to follow up. We purchased all 6 candidate inhibitors of *Pa*DsbB1 and 19 of *Mt*VKOR (Fig. 3 and Experimental procedures) and tested the resupplied molecules again in our agar assay using a collection of *E. coli* strains expressing different DsbB or VKOR homologs (Landeta *et al.,* 2015) in order to determine the MBC, i.e. the minimal concentration to give a pale blue color in agar plates indicative of inhibition of the disulfide bond formation machinery (Fig. 1). We then ranked the inhibitors by potency for each one of the strains (Fig. 4), and observed that most of the *P. aeruginosa* DsbB1 inhibitors also inhibited the *E. coli* DsbB as well as *H. influenza, F. tularensis* and *A. baumannii* DsbB homologs but not the rest of the homologs used in our previous study (Landeta *et al.,* 2015). Compound PA4, which is similar in structure to PA5 and to the anticoagulant warfarin, also inhibited *Rn*VKOR. On the other hand, some VKOR inhibitors found using *M. tuberculosis* VKOR also inhibited *Rn*VKOR and *S. typhymurium* DsbI. A few of them inhibited *F. tularensis* and *A. baumannii* DsbB (Fig. 4).

Inhibition of PaDsbB1 and PaDsbB2 in P. aeruginosa

We tested the effect of *Pa*DsbB1 inhibitors obtained in the HTS with *P. aeruginosa*. In previous work, we found that the *E. coli* disulfide bond formation enzymes are dispensable under aerobic growth but essential for anaerobic growth. This property allowed us to validate *Ec*DsbB inhibitors under anaerobic growth (Landeta *et al.,* 2015; Meehan *et al.*, 2017a). Thus, we determined whether Dsb proteins are also essential anaerobically in *P. aeruginosa*. The two known essential proteins that are substrates of the DsbAB pathway in *E. coli* are the cell division protein, FtsN and lipopolysaccharide transport protein, LptD (Meehan et al., 2017a; 2017b). Even though *P. aeruginosa* lacks FtsN homologs, it has an LptD homolog with six cysteines and four of them are conserved with *Ec*LptD, presumably connected by disulfide bonds. We thus investigated the essentiality of the disulfide bond formation in *P. aeruginosa* growing Δ*dsbA1A2* and Δ*dsbB1B2* mutants under anaerobic conditions (Experimental procedures). Unlike *E. coli*, both mutants were able to grow anaerobically after several passages in M63 minimal media supplemented with 0.2% glucose and 0.2% casamino acids, which precluded our ability to test *Pa*DsbB1 inhibitors using this assay.

We then assayed the activity of the virulence factor elastase since Δ*dsbA1* and Δ*dsbB1B2* mutants

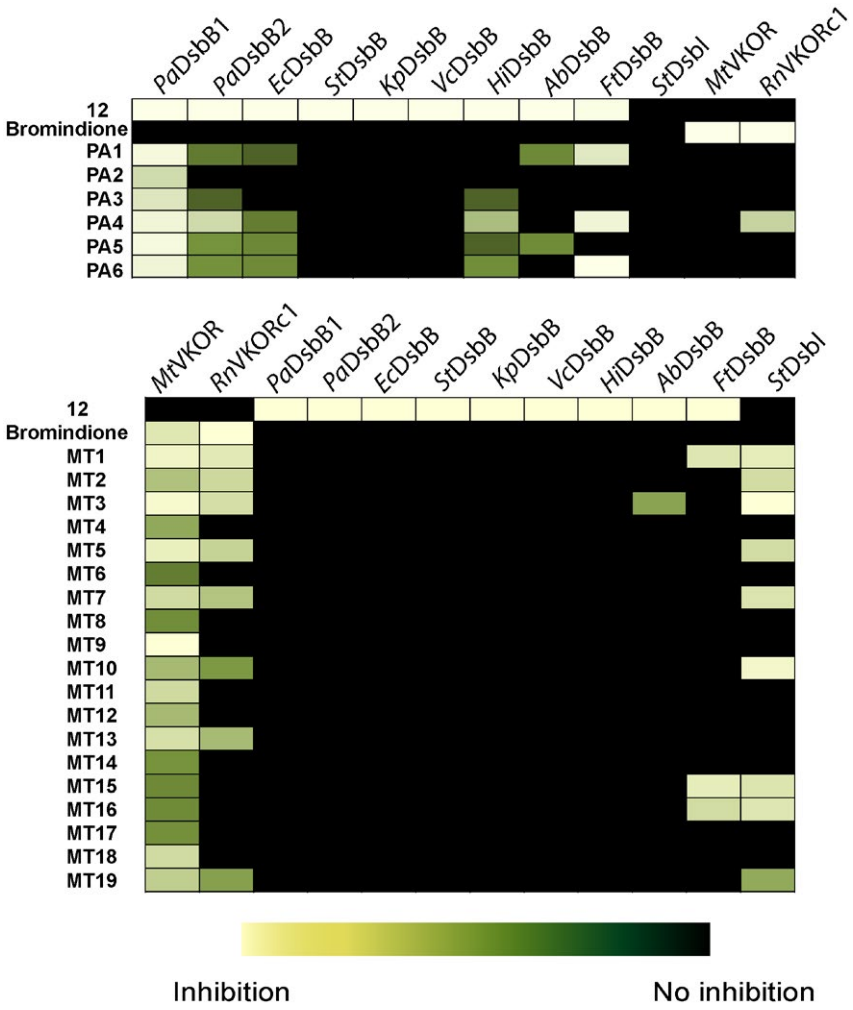

Fig. 4. *In vivo* inhibition of DsbB enzymes from Gram-negative bacteria expressed in *E. coli*. *E. coli dsbB* mutant strains expressing β-Gal^{dbs} and *dsbB* genes from *Salmonella enterica* sv. Typhimurium (*St*), *Klebsiella pneumoniae* (*Kp*), *Vibrio cholerae* (*Vc*), *Hemophilus influenzae* (*Hi*), *Pseudomonas aeruginosa* (*Pa*), *Acinetobacter baumannii* (*Ab*), *Francisella tularensis* (*Ft*) as well as two DsbB-homologs of *P. aeruginosa* (*Pa*) and *S. enterica* sv. Typhimurium (*dsbI*) and two *vkor* genes from *Mycobacterium tuberculosis* (*Mt*) and *Rattus norvegicus* (*Rn*) were tested against resupplied compounds found in HTS as candidate inhibitors. Inhibition range from strong to weak is relative to each DsbB/VKOR-expressing strain and was obtained by dividing the MBC of each compound between the lowest MBC observed for each particular strain (See Supplementary Table 5 for raw data). Results are the average of three independent experiments. Compounds that did not inhibit at the highest concentration tested are shown as black. Strains used in screening are in the first columns of both tables. In order to have a more sensitive counter screening in each case, we used for *Pa*DsbB1 hits (top) a strain expressing low levels of *Mt*VKOR (DHB7657), while for *Mt*VKOR hits (bottom) a strain expressing low levels of *Ec*DsbB was used (DHB7935).

secrete an inactive elastase (Braun *et al.,* 2001; Urban *et al.,* 2001; Arts *et al.,* 2013). We measured elastase (LasB) activity in the supernatant of cells grown in minimal media using a protease substrate that gives a low fluorescence signal. After cleavage of the peptide by LasB the fluorescent donor group cannot transfer the energy to the quenching acceptor group resulting in a high fluorescence signal, which is directly related to the enzymatic activity (Rust *et al.,* 1994; Cathcart *et al.,* 2009). Given that we observed low or no elastase activity in the supernatant of both Δ*dsbA1* and Δ*dsbB1B2* mutants (Fig. 2A), we used this assay to determine DsbB inhibition in *P. aeruginosa* by scaling down the assay to 96-well plates and testing the *Pa*DsbB1 inhibitors against three *P. aeruginosa* strains: wild type, Δ*dsbB1* and Δ*dsbB2* mutants. The strains were grown for 15 h in M63 minimal media in the presence of inhibitors and the supernatants of those cultures were used to determine the amount of active elastase being produced. The IC_{50}s were then calculated comparing the activity observed when the cells were grown in the absence of inhibitor. In addition to the six hits found in HTS, we also tested two pyridazinone-related molecules, compound 12 and 36, found in our previous

work since these molecules showed potency in inhibiting several DsbB homologs from Gram-negatives including *Pa*DsbBs (Landeta *et al.,* 2015; 2017). We found that all compounds except PA2 and PA5 decreased elastase activity of the Δ*dsbB1* and Δ*dsbB2* mutants (Table 1, Columns 3 and 4). Overall these compounds showed inhibitory activity at lower inhibitory concentrations for the Δ*dsbB1* mutant than the Δ*dsbB2* mutant. The fact that all the compounds except PA2 and PA5 showed activity in the Δ*dsbB1* mutant indicates that the compounds target DsbB2 of *P. aeruginosa,* which is the only *dsbB* present in the mutant strain. The same was observed for the Δ*dsbB2* mutant but higher concentrations of the compounds were required to see inhibitory activity, especially for compounds PA1 and PA4. Similarly, this indicates that the compounds also inhibited DsbB1 of *P. aeruginosa,* which is the only DsbB enzyme present in the Δ*dsbB2* mutant and the enzyme used to find these inhibitors by HTS. The inhibition of elastase activity in wild-type cells required even higher concentrations of compounds than those required for either mutant strain, presumably due to the presence of two DsbB proteins (Table 1, Column 2).

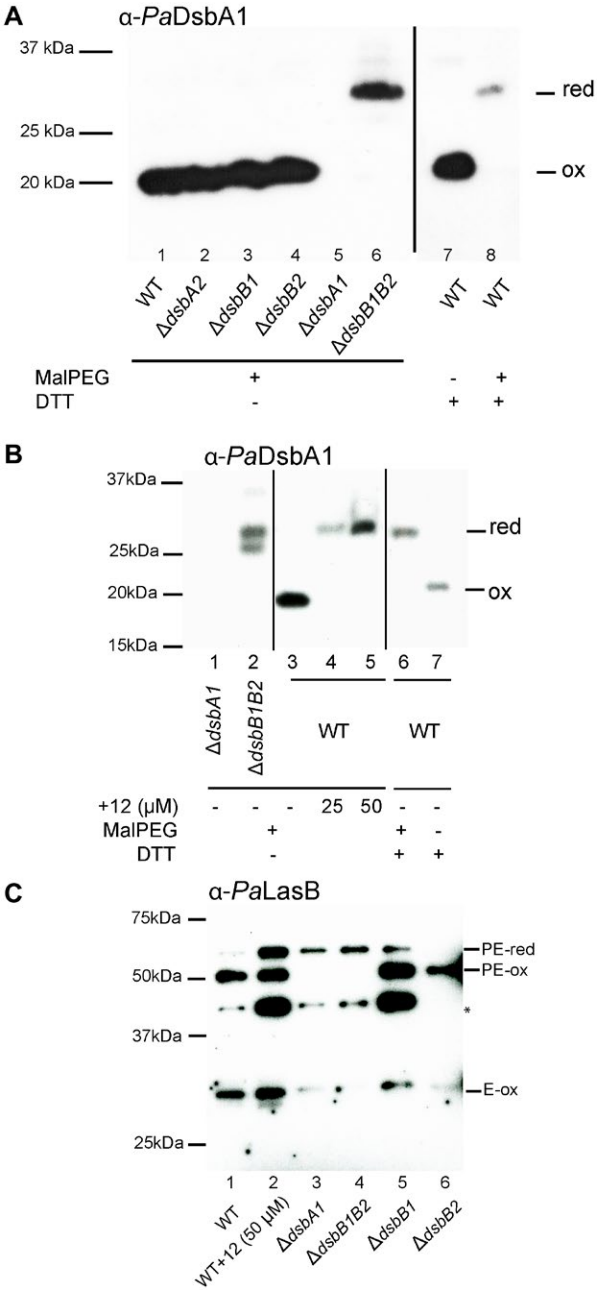

Fig. 5. *In vivo* accumulation of reduced *Pa*DsbA1 (*Pa*DsbB1 and *Pa*DsbB2 substrate) and *Pa*LasB (*Pa*DsbA1 substrate) caused by compound 12.
A. *In vivo* redox states of *Pa*DsbA1 in wild type and mutants. Cells were grown aerobically in M63 minimal media and TCA-precipitated proteins were alkylated with 12.5 mM of MalPEG-2 kDa. Samples were run by SDS-PAGE and immunoblotted with α-*Pa*DsbA1 antibody. Dithiothreitol (DTT) was used for reducing disulfide bonds in controls.
B. *In vivo* redox states of *Pa*DsbA1 in wild-type cells grown in the presence of compound 12. Samples were processed as above.
C. *In vivo* redox states of *Pa*LasB in wild-type cells grown in the presence of compound 12 and in mutants. Cells were grown aerobically in M63 minimal media and precipitated proteins from the supernatant were alkylated with 20 mM of NEM. Samples were analyzed by SDS-PAGE and immunoblotted with α-*Pa*LasB antibody. ox: oxidized, refers to the position of the oxidized protein which is the same as that of the reduced protein with no alkylating agent present; red: reduced, refers to bands where the positions of the protein with reduced cysteines are detected because of the alkylation which adds to the molecular weight; PreLasB: pre-elastase; LasB: elastase; *: degraded Pre-LasB. Blots show representative results from at least two independent experiments.

In addition, we assessed the *in vivo* redox state of DsbA1 and LasB in *P. aeruginosa* grown in the presence of compound 12 in order to determine whether the inhibition of LasB activity was due to accumulation of reduced DsbA (the direct substrate of DsbB1 and DsbB2) and reduced LasB (the direct substrate of DsbA1). We grew cells in M63 minimal media, precipitated the proteins and alkylated them with MalPEG2k and NEM, respectively, to distinguish the reduced and oxidized forms of each protein. Both DsbB1 and DsbB2 are able to re-oxidize DsbA1 since Δ*dsbB1* and Δ*dsbB2* mutants show DsbA1 in oxidized form (Fig. 5A, lanes 3 and 4). However, in the absence of both *dsbB1* and *dsbB2*, DsbA1 accumulates in the reduced state (Fig. 5A, lane 6). These results are in agreement with previous studies (Arts *et al.,* 2013). Similarly, when wild-type cells are incubated with 25 and 50 μM of compound 12, they also show accumulation of DsbA1 in the reduced state (Fig. 5B), which is consistent with compound inhibition of both DsbB1 and DsbB2. When we investigated the redox state of elastase in the supernatant of cell cultures, most of pre-elastase (PE) in the Δ*dsbB1* and Δ*dsbB2* mutants existed in the oxidized state with a small amount in the

mature form (Fig. 5C, lanes 5 and 6), while both Δ*dsbA1* and Δ*dsbB1B2* show pre-elastase in the reduced state and with very little mature elastase (Fig. 5C, lanes 3 and 4). This is also consistent with previous findings of the Δ*dsbA1* mutant (Braun *et al.,* 2001). When wild-type cells are incubated in the presence of 50 μM compound 12, we observe accumulation of pre-elastase in both reduced and oxidized states and similar levels to wild type of mature elastase. There is also a prominent band that runs below pre-elastase and does not correspond to any other reported forms, which may be a degradation product of pre-elastase. This band is more prominent when DsbB1 is mutated or when the cells are treated with compound 12 (Fig. 5C, lanes 5 and 2). Altogether these results indicate that there is accumulation of reduced DsbA1 and reduced pre-elastase when wild-type cells are incubated with compound 12, a *Pa*DsbB1 and *Pa*DsbB2 inhibitor.

In order to assess *in vitro* inhibition of the *Pseudomonas* DsbBs, we purified the enzymes DsbB1, DsbB2 as well as DsbA1 enzymes from *P. aeruginosa*. We then measured the DsbB's activity in oxidizing DsbA using a quinone reduction assay (Regeimbal *et al.,* 2003), calculating IC_{50} and K_i for each inhibitor (Table 1, columns 5–8). We also tested these inhibitors in the same assay but using *E. coli* DsbB and DsbA (Table 1, columns 9–10). Overall, the IC_{50}s of *P. aeruginosa* DsbB1 and DsbB2 were similar. With the exception of PA1, all the compounds were effective against both DsbB1 and DsbB2. All compounds showed activity against *E. coli* DsbB as well, but the potency of these compounds was not as high as compounds 12 and 36. Note that these two pyridazinone-related molecules were found after several rounds of SAR studies and thus inhibitors found in the HTS reported here were expected to be less active than these two compounds (Landeta *et al.,* 2015; 2017).

In order to determine whether the *Pseudomonas* inhibitors obtained in the HTS could have off-target effects on enzymes with thiol-redox activity, we assayed for inhibition of the thiol-redox enzyme, human PDI. The assay measures PDI activity *in vitro* by its ability to reduce insulin. We found that compounds PA2, PA3, PA4 and PA6 inhibited PDI's activity (Table 1, Column 11). These four compounds together with PA4, which inhibited the *Rn*VKOR expressed in *E. coli* (Fig. 4), allowed us to select PA1 as a candidate to follow up in inhibitor development since PA1 does not target human PDI or *Rn*VKOR and it is active in *P. aeruginosa*.

Inhibition of MtVKOR in M. tuberculosis

We assessed the effect of *Mt*VKOR inhibitors obtained in the HTS on *M. tuberculosis* growth using the H37Rv strain as previous results showed that VKOR is essential in this strain (Sassetti and Rubin, 2003; Dutton *et al.,* 2010). We determined MIC for all our 19 candidates and bromindione. With the exception of compounds MT11, MT12, MT15 and MT16, all inhibited growth of wild-type *M. tuberculosis* in the low to high micromolar range (Table 2, Column 2).

In order to obtain more evidence that the remaining MT inhibitors were acting in *M. tuberculosis* directly on VKOR, we constructed a conditionally lethal strain. To this end, we used a CRISPRi (CRISPR interference) platform to knock down *vkor* in *M. tuberculosis* (Rock *et al.,* 2017). The system allows transcriptional repression using a *Streptococcus thermophilus* nuclease-dead Cas9 ($dCas9_{Sth1}$) under the control of a Tet promoter and a ~20 bp targeting region into the single guide RNA (sgRNA) scaffold. One of the advantages of this methodology is that it is tunable either by varying the targeted PAM (Protospacer Adjacent Motif within the target DNA sequence) 'strength' or by varying the concentration of the $dCas9_{Sth1}$ inducer, ATc (Rock *et al.,* 2017). Such a system allowed us to express the minimal amount of *vkor* necessary for growth, thus sensitizing the strain to potential VKOR inhibitors. We constructed several CRISPRi vectors with different PAM sequences and transformed them into *M. tuberculosis*. We then tested the growth of the resulting strains under inducing and non-inducing conditions of $dCas9_{Sth1}$ (Supplementary Fig. 6). The *vkor*-silenced strains were defective in growth in 7H9 media when CRISPRi is induced and the growth defect correlated with the PAM strength and the ATc concentration (Rock *et al.,* 2017). We selected the JR1740 strain, which displays low PAM strength side with high concentrations of $dCas9_{Sth1}$ inducer (Supplementary Fig. 6) and partial growth. We determined the protein levels of VKOR in *M. tuberculosis* JR1740 cell lysates by immunoblotting using an anti-VKOR antibody (Fig. 6). This strain has a ~4-fold decrease in VKOR levels compared to a wild type or non-induced parental strain and a twofold decrease in growth as measured by absorbance at 600 nm (A_{600}), which is indicative of the essentiality of this gene in *M. tuberculosis* (Fig. 6). We then used this knockdown strain to test our *Mt*VKOR inhibitors. If any of the candidate molecules inhibit VKOR, they should display lower MICs in a strain that produces less VKOR (induced with ATc) than a strain on which VKOR levels are comparable to wild-type levels (non-induced). Five inhibitors did indeed show lower MICs (MT1, MT2, MT3, MT7 and MT17) than those observed for the non-induced strain (Table 2, column 3). For reasons that are unclear the VKOR knockdown strain displayed more resistance to compounds MT4, MT18 and MT19, opposite to what we expected. Even though more experiments are needed to explain these results, one could speculate these drugs may be targeting another essential process that is not

Table 2. Analysis of *Mt*VKOR inhibitors.

ID	*In vivo assay* (MIC, μM)[a]	Fold change	***In vitro*** assay[c]		PDI[d]
		Knockdown[b]	IC_{50} (μM)	Ki (μM)	IC_{50} (μM)
Bromindione	250 ± 0	1	5 ± 0.73	1 ± 0.09	N
MT1	50.5 ± 0	6.66	ND	ND	N
MT2	26.04 ± 9	32.01	5 ± 0.5	4 ± 0.3	N
MT3	21.68 ± 0	2	4 ± 0.25	2.5 ± 0.1	233.1 (160.1–339.4)
MT4	575.2 ± 0	0.49	ND	ND	68.12 (30.13–154.0)
MT5	125 ± 0	1	ND	ND	N
MT6	138 ± 0	1	ND	ND	N
MT7	41 ± 0	3.46	ND	ND	N
MT8	114.5 ± 0	1	20 ± 2.5	9 ± 1	N
MT9	>979 ± 0	–	3 ± 0.5	2 ± 0.05	N
MT10	25.83 ± 11.2	1	ND	ND	N
MT11	>309.6 ± 0	–	ND	ND	N
MT12	>166 ± 0	–	ND	ND	7.61 (3.397 to 17.08)
MT13	30.25 ± 0	1	ND	ND	N
MT14	169 ± 0	1	ND	ND	N
MT15	>523 ± 0	–	ND	ND	339.5 (82.64 to 1394)
MT16	>521.6 ± 0	–	ND	ND	N
MT17	7.46 ± 0	2	11 ± 1.1	5 ± 0.25	N
MT18	0.4 ± 0.17	0.005	ND	ND	N
MT19	0.5 ± 0	0.125	9 ± 1	3 ± 0.5	291.6 (114.4–743.6)

Abbreviations: ND: Not determined. N: No inhibition observed up to 100 μM.

Data represent the average of at least two independent experiments with 95% confidence intervals in parenthesis or ±SD.

[a]*In vivo* inhibition was done by growth inhibition using an alamar blue assay.

[b]Fold change was determined using *M. tuberculosis* JR1740 strain in which CRISPRi is induced with ATc. The MIC was determined by triplicate using alamar blue assay and the fold change was determined by dividing the MIC of the strain grown without ATc (non-induced) to the MIC of the strain grown with 500 ng mL^{-1} of ATc (induced). Fold change was not calculated for compounds that did not inhibit growth at the highest concentration tested.

[c]*In vitro* inhibition was measured by following the reduction of ubiquinone with purified His-tagged enzymes. The assay used 10 nM of *Mt*VKOR with 20 μM reduced-*Ec*DsbA and 25 μM Ubiquinone-1. For K_i determination 1–100 μM of Ubiquinone-1 was used.

[d]PDI activity was measured using the insulin reduction assay.

relevant to the cell when growing slowly, such as when VKOR levels are decreased.

We chose 6 *Mt*VKOR inhibitors to test their effects *in vitro* with purified *Mt*VKOR and *Ec*DsbA using a ubiquinone reduction assay (Table 2, Columns 4 and 5). We selected compounds that were in the low (MT17 and MT19), medium (MT2 and MT3) and high (MT8) micromolar range of *M. tuberculosis* growth inhibition and one that did not inhibit at the highest concentration tested (MT9) (Table 2, Column 2). All these compounds showed an IC_{50} in the range of 3 to 20 μM when *Mt*VKOR oxidizes reduced *Ec*DsbA using ubiquinone-1. In this assay, MT9 displayed an IC_{50} of 3 ± 0.5 μM but has no effect on growth of *M. tuberculosis* at concentrations up to and including 979 μM, suggesting that the drug is not targeting *Mt*VKOR in *M. tuberculosis* while it targets *Mt*VKOR when expressed in *E. coli*, in which the MIC is 0.44 μM (Fig. 3). This may be due to the drug being metabolized by *M. tuberculosis* as observed with other molecules (Awasthi and Freundlich, 2017) or the drug may target *Mt*VKOR when partnered with *Ec*DsbA rather than with *Mt*DsbA. Unfortunately, our attempts to use *Mt*DsbA in the ubiquinone reduction assay with *Mt*VKOR showed very low activity, precluding our ability to measure inhibition using both mycobacterial proteins.

Similarly to *Pa*DsbB1 inhibitors, we used PDI *in vitro* assay to determine off-target effects. We found that compounds MT3, MT4, MT12, MT15 and MT19 inhibited PDI (Table 2, Column 6), while compounds MT1, MT2, MT3, MT5, MT7, MT10, MT13 and MT19 inhibited the *Rn*VKOR expressed in *E. coli* (Fig. 4). Thus, MT17 is the only compound that did not inhibit human PDI nor *Rn*VKOR, is active in *M. tuberculosis* and displays a twofold change in the MIC of the *M. tuberculosis* knockdown strain, making this compound a candidate to follow up in inhibitor development.

Discussion

The animal studies presented here provide evidence that the *dsbB1B2* double mutant and *dsbA1* mutant of *P. aeruginosa* are defective in virulence in two mice infection models, pneumonia and keratitis. Animal experiments with the *dsbA1* mutant showed slightly larger defects in the lungs than the *dsbB1B2* double mutant, while in the eye model both mutant strains were similarly affected. This is not surprising as it is well known that DsbA mutants confer greater defects in disulfide bond formation than DsbB mutants, presumably because some degree of oxidation of DsbA takes place in the presence of oxygen (Meehan *et al.*, 2017a). These animal studies, along with the availability of a sensitive assay for screens, provide additional reason to consider that the search for inhibitors of bacterial DsbBs may yet yield candidates for antibacterial development.

In an attempt to demonstrate inhibition of *M. tuberculosis* VKOR we have used a CRISPR-dCas9 system to generate knockdown strains of the essential gene *vkor* (Rock *et al.,* 2017). Similar to previous studies, we observed that the silencing of VKOR affects the growth of *M. tuberculosis* (Sassetti and Rubin, 2003; Dutton *et al.,* 2010). We anticipate that these knockdown strains will allow the study of disulfide bond formation in *M. tuberculosis* and may allow for identification of the essential substrates of the pathway.

Our HTS presented in this work allowed detection of inhibitors of the DsbB1 enzyme of *P. aeruginosa* and VKOR enzyme of *M. tuberculosis* when each of them is expressed in an *E. colidsbB* mutant strain. The HTS based on a sensitive assay, has yielded inhibitors that then were shown to also inhibit the enzymes purified from their native organism, and to interfere with disulfide bond formation in *P. aeruginosa* cultures and with the growth of *M. tuberculosis*. In the case of *Pa*DsbB1 inhibitors, we have used an indirect assay to measure DsbB inhibition by measuring elastase activity in the supernatant of cell cultures. Since elastase is a substrate of the disulfide bond formation pathway in *P. aeruginosa*, its activity is decreased in *dsbA1* and *dsbB1B2* mutants. For *Mt*VKOR inhibitors, we have made use of one of the knockdown strains to determine the synergy of the growth defect with *Mt*VKOR inhibitors as one way to demonstrate that the small molecules target *Mt*VKOR. While there are many factors affecting enzyme inhibition, we have observed in 6 out of 19 molecules a 2- to 32-fold reduction in the MIC using the knockdown strain, thus helping us prioritize the molecules for further study.

A potential strength of our screen is its selectivity. We observed an unusually low hit rate in the *Pa*DsbB1 screen with a large sample of molecules (~200,000 compounds) similarly to what we observed in our previous screen with *Ec*DsbB (~50,000 compounds) (Landeta *et al.,* 2015). The hit rates of DsbB proteins are in the range of 0.01% (Supplementary Table 1) to 0.02% (Landeta *et al.,* 2015). For the *Mt*VKOR screens, the hit rate dropped 5-fold when we used a strain that more efficiently complements the *E. colidsbB* mutant (0.057% vs 0.29%, Supplementary Table 1) (Landeta *et al.,* 2015). This observation is consistent

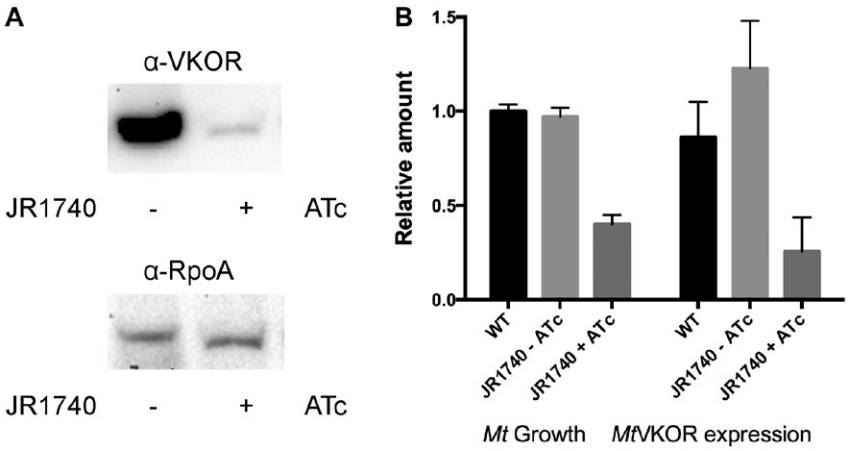

Fig. 6. Knocking down disulfide bond forming enzyme VKOR in *M. tuberculosis* causes a growth defect.
A. *M. tuberculosis* knockdown JR1740 strain shows reduced levels of VKOR when CRISPRi is induced with ATc. *M. tuberculosis* wild type and JR1740 strains were diluted to an A_{600} of 0.005 and grown in 7H9 media without or with 500 ng mL^{-1} of ATc at 37°C for seven days. Cells were lysed and extracts were filtered twice, then proteins were TCA precipitated and quantified by Pierce-BCA method. 50 µg of total protein were run in 12% acrylamide gels and transferred to PVDF membranes to be immunoblotted against anti-*Mt*VKOR antibody or anti-RpoA.
B. *M. tuberculosis* knockdown JR1740 strain shows a decrease in growth and reduced levels of VKOR when CRISPRi is induced with ATc. *M. tuberculosis* wild type and JR1740 strains were diluted to an A_{600} of 0.005 and grown in 7H9 media without or with 500 ng mL^{-1} of ATc at 37°C for seven days. The relative amount of *M. tuberculosis* growth was calculated comparing the final A_{600} of JR1740 strain ± ATc to the A_{600} of wild-type strain. The relative intensity of *Mt*VKOR bands was estimated by ChemiDoc-XRS using wild type as a reference band. Data represent the average of at least three independent experiments ± SD

with our hypothesis that the much higher rate of hits is explained by the lower effectiveness of oxidation of DsbA, which we overcame significantly by overexpressing *Mt*VKOR (Supplementary Fig. 4).

Contrary to what we observed with pyridazinone-related molecules such as compounds 12 and 36 (Landeta *et al.,* 2015; 2017), the *Pa*DsbB1 inhibitors found in the HTS did not inhibit the DsbBs from *Salmonella enterica* sv Typhimurium, *Klebsiellapneumonia* or *Vibrio cholerae*. Similarly, most of the *Mt*VKOR inhibitors targeted only *Rn*VKOR but not DsbB enzymes in *E. coli*, with the exception of *S. enterica* sv typhimurium DsbI, an atypical DsbB homologue that together with DsbL (a DsbA homologue) is dedicated to oxidize arylsulfate-sulfotransferase in *S. enterica* (Lin *et al.,* 2009; Heras *et al.,* 2010). Thus, overall these molecules show selectivity toward either DsbB or VKOR enzymes. We also found no *in vitro* inhibition of PDI for 2 out of 6 *Pa*DsbB1 inhibitors and 16 out of 20 *Mt*VKOR inhibitors, which also shows some degree of selectivity among thiol-redox enzymes. The promiscuity of pyridazinone-related molecules toward DsbB enzymes but not toward other thiol-redox enzymes with catalytic cysteines (such as VKOR, DsbA or PDI) is explained by the particular mechanism of action of this class of compounds. We previously demonstrated that pyridazinones displace quinone from its binding site on DsbB and react covalently to a conserved catalytic cysteine in the enzyme, thus preventing catalytic turnover. These newly discovered inhibitors of some DsbB enzymes may therefore speak to a shared mechanism of inhibition and the conservation of those residues/structural features with which these compounds interact.

Our studies suggest that compounds PA1 and MT17 are candidates to follow up in the development of more effective inhibitors of *Pa*DsbB and *Mt*VKOR enzymes respectively. For instance, further SAR studies of PA1 and MT17 may improve their effectiveness and help in the understanding of the mechanism of inhibition as we have demonstrated for pyridazinone-related compounds 12 and 36 (Landeta *et al.,* 2015; 2017). While 8 out of 19 *Mt*VKOR inhibitors also inhibited *Rn*VKOR, we think that testing analog structures of these compounds may give more candidates that are selective toward *Mt*VKOR but not *Rn*VKOR. Of particular interest are those molecules that inhibited growth of *M. tuberculosis* and showed a change in MIC with the VKOR-silenced strain, such as compounds MT2 and MT7. In agreement with this, we have observed that molecules structurally related such as compound MT8, PA4 and PA5 (which are also structurally related to the anticoagulant warfarin) display different activity against *Rn*VKOR and *Mt*VKOR. This suggests that modifying groups at the core structure, in this case coumarin, gives selectivity toward one enzyme or the other. Overall, these molecules represent a starting point for chemical modifications in order to improve their potency and selectivity as well as to unravel their mechanisms of inhibition.

Experimental procedures

Bacterial strains and growth conditions

The strains and plasmids used in this study are listed in Table 3. Strains and growth conditions used for screening were done as described previously (Landeta *et al.,* 2015). The *E. coli* screening strain of *Pa*DsbB1 was constructed by site-directed mutagenesis of the –10 box of *Trc* promoter in pCL25 plasmid (Landeta *et al.,* 2015) in order to convert the plasmid from pDSW204 to pDSW206. The resulting plasmid (pLEM6) was transformed into HK325 and this strain (CL523) was used in X-Gal plates without the addition of IPTG. The *E. coli* screening strain of *Mt*VKOR was constructed by transforming pRD33 into HK325 (CL382), since our original VKOR screening strain (DHB7657) (Landeta *et al.,* 2015) did not completely restore DsbB activity, giving rise to colonies with a pale blue color on X-Gal plates. The conditions used for CL382 strain in X-Gal plates required the addition of 25 μM of IPTG. FSH250 strain was used with 300 μM IPTG and 60 μg mL^{-1} of X-Gal instead of the 120 μg mL^{-1} used for all the other strains (Hatahet *et al.,* 2015). *P. aeruginosa* clean deletion mutants were constructed using overlap extension PCR and homologous recombination as described before (Horton, 1993). The deletion of the targeted genes was confirmed by PCR amplification and sequencing. Plasmids used to complement *P. aeruginosa* mutants were constructed cloning the gene and the upstream region containing the promoter (500 bp upstream) using EcoRI-XmaI sites for *dsbB1* (pCL84) and XbaI-SacI sites for *dsbB2* (pCL85). For *dsbA* genes the *dsbA1* promoter (500 bp upstream *dsbA1*) was cloned in NheI-EcoRI sites and then EcoRI-XmaI sites were used to clone *dsbA1* (pCL119) or *dsbA2* (pCL120) genes. The resulting plasmids were verified by sequencing and transformed in *P. aeruginosa* mutants and strains were tested in twitching motility to determine restoration of the mutant phenotype. All *E. coli* strains were grown in NZ or M63 0.2% glucose either liquid or agar media at 30°C when indicated. All *P. aeruginosa* strains were grown in LB or M63 0.2% glucose at 37°C. The antibiotic concentrations used were: ampicillin 100 μg mL^{-1}, kanamycin 40 μg mL^{-1} and chloramphenicol 10 μg mL^{-1}, gentamicin 15 μg mL^{-1} for *E. coli* or 75 μg mL^{-1} for *P. aeruginosa*.

P. aeruginosa growth under anaerobiosis

To prepare anaerobic media, M63 supplemented with 0.2% glucose, 0.2% casamino acids and 40 mM KNO_3 was boiled and incubated for two days in a Coy anaerobic chamber containing 85% nitrogen, 10% carbon dioxide and 5% hydrogen (Meehan *et al.*, 2017a). Then, 5 mL of this media were dispensed in glass tubes sealed with plastic caps to maintain anaerobiosis outside the anaerobic chamber. *P. aeruginosa* strains Δ*dsbA1* (CL384), Δ*dsbA1A2* (CL541), Δ*dsbB1B2* (CL356) and wild type were grown aerobically overnight in LB, washed with PBS buffer and injected with

Table 3. Strains and plasmids.

Strain	Genotype	Ref.
E. coli strains		
BL21 (DE3)	*huA2 [lon] ompTgal* (λ DE3*) [dcm]* Δ*hsdS*	NEB
	λ DE3 = λ *sBamHIo*Δ*EcoRI-B int::(lacI::PlacUV5::T7 gene1) i21* Δ*nin5*	
JR6 (FSH94)	C43 (DE3) Δ*dsbB* (Km^r)	Regeimbal *et al.* (2003)
NT	C43 (DE3) Δ*dsbB* (Km^r) pLysS	This study
HK295	MC1000 Δ*ara*714 *leu+*	Kadokura and Beckwith (2002)
HK320	HK295 Δ*dsbB*	Kadokura and Beckwith (2002)
HK325	HK295 Δ*dsbB* λ*att*::*malF-lacZ*102 (Km^r)	Kadokura H.
DHB7935	HK295 Δ*dsbB*λ*att*::*malF-lacZ*102 (Km^r) ϕ80::pDSW206dsbB (Amp^r)	Landeta *et al.* (2015)
DHB7657	HK295 ΔdsbB λ*att*::*malF-lacZ*102 (Km^r) pTrc99a*Mt*VKOR (Amp^r) *recA*::Cm^r	Landeta *et al.* (2015)
CL320	HK295 λ*att*::*malF-lacZ*102 (Km^r) Δ*dsbB*::$_{Trc204promoter}$-*KpdsbB* (Amp^r)	Landeta *et al.* (2015)
CL377	HK295 Δ*dsbB*λ*att*::*malF-lacZ*102 (Km^r) pDSW204*PadsbB2* (Amp^r)	Landeta *et al.* (2015)
CL378	HK295 Δ*dsbB*λ*att*::*malF-lacZ*102 (Km^r) pDSW204*AbdsbB* (Amp^r)	Landeta *et al.* (2015)
CL369	HK295 Δ*dsbB*λ*att*::*malF-lacZ*102 (Km^r) pDSW204*StdsbB* (Amp^r)	Landeta *et al.* (2015)
CL368	HK295 Δ*dsbB*λ*att*::*malF-lacZ*102 (Km^r) pDSW204*StdsbI* (Amp^r)	Landeta *et al.* (2015)
CL373	HK295 Δ*dsbB*λ*att*::*malF-lacZ*102 (Km^r) pDSW204*VcdsbB* (Amp^r)	Landeta *et al.* (2015)
CL370	HK295 Δ*dsbB*λ*att*::*malF-lacZ*102 (Km^r) pDSW204*FtdsbB* (Amp^r)	Landeta *et al.* (2015)
CL371	HK295 Δ*dsbB*λ*att*::*malF-lacZ*102 (Km^r) pDSW204*HidsbB* (Amp^r)	Landeta *et al.* (2015)
CL379	HK295 Δ*dsbB*λ*att*::*malF-lacZ*102 (Km^r) pDSW204 (Amp^r)	Landeta *et al.* (2015)
FSH250	HK295 Δ*dsbB* λ*att*::*malF-lacZ*102 (Km^r) Δ*metL*::FRT $HslV_{C160Y}$ $YidC_{T362I}$ Δ*tnaA*::CAT (Cm^r) pTrc99a-*Rn*VKORc1 ΔA_{31}AR (pJBL420.1, Amp^r)	Hatahet *et al.* (2015)
CL382	HK295 Δ*dsbB*λ*att*::*malF-lacZ*102 (Km^r) pTrc99a-6XHis*Mt*VKOR (Amp^r)	This study
CL523	HK295 Δ*dsbB* λ*att*::*malF-lacZ*102 (Km^r) pDSW206*PadsbB1* (Amp^r)	This study
P. aeruginosa strains		
PA14	*P. aeruginosa* UCBP-PA14	Lory Lab collection
CL384	*P. aeruginosa* Δ*dsbA1* (PA14_72450)	This study
CL339	*P. aeruginosa* Δ*dsbB1* (PA14_07000)	This study
CL355	*P. aeruginosa* Δ*dsbB2* (PA14_69400)	This study
CL356	*P. aeruginosa* Δ*dsbB1* Δ*dsbB2*	This study
CL540	*P. aeruginosa* Δ*dsbA2* (PA14_59960)	This study
CL541	*P. aeruginosa* Δ*dsbA1* Δ*dsbA2*	This study
CL725	*P. aeruginosa* Δ*dsbA1* Δ*dsbA2* (CL541) pJN105-$_{PdsbA1}$-*PadsbA1* (pCL119, Gm^r)	This study
CL726	*P. aeruginosa* Δ*dsbB1* Δ*dsbB2* (CL356) pJN105-$_{PdsbB1}$-*PadsbB1* (pCL84, Gm^r)	This study
M. tuberculosis strains		
WT	*M. tuberculosis* H37Rv	Rubin Lab collection
JR1740	*M. tuberculosis* pJR1740 inserted into L5 attachment site	This study
Plasmids		
pTrc99a	Expression vector, Amp^r	Amann *et al.* (1988)
pDSW206	Promoter down mutation in –10 and –35 of pTrc99A	Weiss *et al.* (1999)
pDSW204	Promoter down mutation in –35 of pTrc99A	Weiss *et al.* (1999)
pJN105	Broad-host-range cloning vector with araC-P_{BAD} (Gm^r)	Newman and Fuqua (1999)
pET28a	Expression vector, T7lac promoter, N-terminal and C-terminal His tag, thrombin cleavage site, pBR322 origin, Km^r	EMD
pET23a	Expression vector, T7lac promoter, C-terminal His tag, thrombin cleavage site, pBR322 origin, Amp^r	EMD
pLysS	pACYC184-P_{Tet}T7 lysozyme gene (at BamHI), p15A origin (Cm^r)	Novagen
pRD33	pTrc99a-6XHis-*Mtvkor* (Amp^r)	Dutton *et al.* (2008)
pCL25	pDSW204*PadsbB1* (Amp^r)	Landeta *et al.* (2015)
pLEM6	pDSW206*PadsbB1* (Amp^r)	This study
pCL84	pJN105-$_{PdsbB1}$-*PadsbB1* (Gm^r)	This study
pCL119	pJN105-$_{PdsbA1}$-*PadsbA1* (Gm^r)	This study
pCL85	pJN105-$_{PdsbB2}$-*PadsbB2* (Gm^r)	This study
pCL120	pJN105-$_{PdsbA1}$-*PadsbA2* (Gm^r)	This study
pJR1740	*Mtvkor* (Rv2968c) sgRNA under constitutive promoter, $dCas9_{Sth1}$ under Tet promoter (Km^r)	This study
pFL39	pET28a-*Ec*DsbA (N' 6His tag, cloned at NdeI-XhoI)	Landeta *et al.* (2015)
pWM76	pQE70-*Ec*$DsbB_{C8A,C49V}$-6His (Amp^r)	Regeimbal *et al.* (2003)
pCL96	pET23a-*Mt*VKOR (C′ 6His tag, cloned at NdeI-XhoI)	This study
pCL97	pET23a-*Mt*$DsbA_{1-255}$ (C′ 6His tag, cloned at NdeI-XhoI)	This study
pCL98	pET23a-ssTorT$_{1-18}$-*Mt*$DsbA_{47-255}$ (C′ 6His tag, cloned at NdeI-XhoI). DsbA's transmembrane segment has been replaced by TorT signal sequence),	This study
pCL99	pET28a-*Mt*$DsbA_{47-255}$ (N' 6His-tag, cloned at NdeI-XhoI, deletion of transmembrane segment)	This study
pNT1	pET23a-*Pa*$DsbA1_{21-211}$ (C′ 6His tag, cloned at NdeI-XhoI)	This study
pNT2	pET23a-*Pa*$DsbB1_{C154Y}$ (C′ 6His tag, cloned at NdeI-XhoI, non-catalytic cysteine mutated)	This study
pNT3	pET23a-*Pa*$DsbB2_{C17A,C53A}$ (C′ 6His tag, cloned at NdeI-XhoI, non-catalytic cysteines mutated)	This study

a syringe into the 5 mL of anaerobic M63 media to an A_{600} of 0.0001 (~10^5 CFU mL^{-1}, bacteria were diluted and enumerated on LB plates). Cultures were incubated for 24 h at 37°C yielding ~10^8 CFU mL^{-1}. About 50 µL of these anaerobic grown cultures were then diluted (~10^6 CFU mL^{-1}) into 5 mL of fresh anaerobic minimal media and grown for 24 h at 37°C, again reaching ~10^8 CFU mL^{-1}. Two additional passages were done with the same results. Therefore, no obvious growth defect was observed after a total of approximately 28 doublings.

High throughput screen of compound libraries

Compound collections were supplied by the Institute of Chemistry and Cell Biology (ICCB) at Harvard Medical School. Libraries different from the previous tested libraries (Landeta *et al.,* 2015) were selected. The screen included 216,767 compounds from several commercial small molecule libraries (Supplementary Table 1). Agar screening plates and 100 nL compound transferred into the agar were done as reported before (Landeta *et al.,* 2015). Final concentration of compounds in screening ranged from 16–25 µM. The compounds that appeared as hits in the first round of screening were confirmed following cherry-picking and re-testing (at final concentration of 15 and 50 µM) using Hewlett Packard D300 dispenser and HPD Digital Dispenser 3.1.2 Premier software (USA). For *Pa*DsbB1 hits two additional strains were tested in the cherry-pick assay, weakened *Mt*VKOR (DHB7657) and *Rn*VKOR (FSH250) to discard molecules that were not targeting specifically *Pa*DsbB1 or can have an anticoagulant side effect. On the contrary for *Mt*VKOR hits, weakened *Ec*DsbB (DHB7935) and *Rn*VKOR (FSH250) were used instead. This allowed us to narrow down the molecules to resupply.

Compound resupply and retest of small molecule inhibitors

Compound 36 was obtained by custom synthesis from Sundia MediTech Company Ltd China, its purity was over 95% when analyzed by NMR and LCMS. Bromindione (sc-396742) was purchased from ChemCruz (USA). Compound 12 (EN300-173996, purity 95%), PA1 (Z56868922), PA2 (Z55331918), PA3 (EN300-43376, purity 95%), PA6 (EN300-03922) MT1 (Z56871780), MT2 (Z56801377), MT5 (EN300-220348) were purchased from Enamine (Ukraine). Compound MT9 (A2385) and MT10 (PHR1686-1G) were purchased from Sigma (USA). Compounds PA4 (JFD02470SC) and PA5 (RJC03767SC) were purchased from Maybridge, Ltd (UK). Compound MT8 (5162526) was purchased from Hit2Lead (USA). Compounds MT15 (G751-2182), MT16 (L466-0343), MT17 (L438-0032), MT18 (L454-0207) and MT19 (D268-0470) were purchased from ChemDiv, Inc (USA). Compounds MT6 (OSSK_695834), MT13 (OSSL_944753) and MT14 (OSSK_748556) were purchased from Princeton BioMolecular Research, Inc (USA). Compound MT3 (19063) was purchased from MolMall Sarl (Switzerland), Compound MT4 (ST014023) from TimTec (USA), MT7 (AG-690/10252054) from Specs (USA), MT11 (MD-0230) from Key Organics, Ltd (UK), MT12 (BML-GR343-0010) from EnzoLife Sciences (USA). All purchased compounds were analyzed by mass spectrometry (LCMS) to verify their molecular weights and to confirm their purity (over 90%). All resupplied molecules were dissolved in DMSO using a wider range of concentrations (often from 50 to 0.5 µM as final concentration) for pin-transfer similar to the process of HTS and tested against the collection of *E. coli* strains to determine MBCs (minimal concentration that causes a pale blue color in the well) as described before (Landeta *et al.,* 2015).

Protein purification and in vitro assays

Inhibitors were evaluated *in vitro* by a ubiquinone-1 (UQ-1) reduction assay at 275 nm. His-tagged DsbB or VKOR enzymes were produced in *E.coli* using fermentation and purification as described before (Regeimbal *et al.,* 2003; Landeta *et al.,* 2015). Purity of proteins was over 90% as determined by SDS-PAGE. Reduced *Pa*DsbA1 or *Ec*DsbA was used as a source of electrons for *Pa*DsbB1/B2 or *Mt*VKOR/*Ec*DsbB respectively. For determination of inhibition constants (IC_{50} and K_I), various amounts of inhibitors were mixed with 10 nM DsbB in 50 mM sodium phosphate buffer (pH 6) containing 300 mM NaCl, 0.2% DDM (Affymetrix Inc.; Santa Clara, CA, USA) and UbQ-1 (Sigma, 1–100 µM). For VKOR, 10% glycerol was added to the buffer and 0.3% DDM was used instead of 0.2%. Reactions were started at room temperature by the addition of small amounts of highly concentrated DsbA solution to give a final concentration of 20 µM. The following enzyme kinetics were determined for *Ec*DsbB: $K_{m(UQ\text{-}1)}$ of 2.1 µM, $K_{m(EcDsbA)}$ of 4.6 µM and k_{cat} of 4.1. For *Pa*DsbB1: $K_{m(UQ\text{-}1)}$ of 3 µM, $K_{m(PaDsbA1)}$ of 3 µM and k_{cat} of 3. For *Pa*DsbB2: $K_{m(UQ\text{-}1)}$ of 2.9 µM, $K_{m(PaDsbA1)}$ of 2.9 µM and k_{cat} of 2.1. For *Mt*VKOR: $K_{m(UQ\text{-}1)}$ of 5.5 µM, $K_{m(EcDsbA)}$ of 7 µM and k_{cat} of 1.1.

PDI insulin reduction assay

PDI enzymatic activity was evaluated using PROTEOSTAT® PDI assay kit (Enzo Life Sciences, Inc., USA) as per manufacturer's instructions. About 1 µL of compounds dissolved in DMSO were added in the final concentrations: 0.5, 10, 50 and 100 µM. 1 µL of DMSO was used instead to determine 100% PDI activity. Bacitracin was used as a positive control and insulin only or insulin with compound was used as negative controls. To follow the kinetics of the reaction, the PROTEOSTAT® PDI stop reagent was substituted by buffer. Plates were incubated in a microplate reader (VERSAmax) for 1 h at room temperature while reading the kinetics of the reaction every 47 s at λ_{ex} 500 nm/λ_{em} 603 nm. For compounds that interfered with PROTEOSTAT® PDI detection reagent, absorbance was used instead of substituting the dye by buffer and A_{650} was read every minute during 1 h. Slopes were calculated with SoftMax®Pro (Molecular Devices, LLC) and used to determine inhibition using PDI with no drug activity as 100% activity. IC_{50} was determined using non-linear log inhibitor vs normalized response with Prism 6 software (GraphPad, La Jolla, USA).

Determination of secreted elastase activity in P. aeruginosa cultures

P. aeruginosa strains were grown in LB overnight, washed with PBS buffer and diluted in M63 containing 0.2% glucose 0.2% casamino acids media to an A_{600} of 0.02. 200 µL aliquots of diluted cultures were placed in 96-well plates with flat-bottom (Greiner Bio-one, Austria) and different concentrations of compounds dissolved in DMSO were added to a final concentration of 0.2% DMSO. Serial two-fold dilutions ranging from 0.195 to 100 µM of drug were tested. Plates were incubated at 37°C and 800 rpm 80% humidity in an orbital shaker (Multitron, ATR). After 15 h of growth, 10 µL of cells were diluted in 90 µL of PBS to read A_{600} in a microplate reader (VERSAmax). All strains grew to a similar A_{600}, see growth curve in Supplementary Fig. 7. Then, the rest of cells were transferred to v-shape 96-well plates (Greiner Bio-one) to centrifuge for 10 min at 3,000 rpm. Aliquots of 10 µL of supernatant were placed into 96-well black plates with clear flat bottom (Corning, Costar) and diluted with 85 µL of 50 mM Tris-HCl pH 7 with 2.5 mM $CaCl_2$ buffer and these dilutions were used to determine elastase activity. The reaction was started with the addition of 5 µL of 5 mM metalloendopeptidase substrate (2-aminobenzoyl-Ala-Gly-Leu-Ala-4-nitrobenzylamide, #SC00185, Sigma USA) to reach a final concentration of 250 µM. Plates were incubated in a microplate reader (VERSAmax) for 1 h at 37°C while reading the kinetics of the reaction every minute at λ_{ex} 320 nm/λ_{em} 430 nm. Slopes were calculated with SoftMax®Pro software (Molecular Devices, LLC) and divided by A_{600} to correlate with growth, these were then used to determine the extent of inhibition using wild-type strain (or Δ*dsbB1 or* Δ*dsbB2*) without inhibitor (only 0.2% DMSO), which activity was considered as 100%. Δ*dsbA* and Δ*dsbB1B2* mutants were used as negative controls since little or no activity (below level of detection, <0.1 µg mL^{-1}/A_{600}) was detected in their supernatants under these conditions. Each concentration of drug was tested by triplicate and used to calculate the IC_{50} (concentration of drug where 50% inhibition of elastase activity is observed compared to no-drug condition) and their 95% confidence intervals using non-linear log inhibitor vs normalized response with Prism 6 software (GraphPad, La Jolla, USA). Amount of elastase in the supernatant of wild type was estimated to be around 127.3 ± 19 µg mL^{-1}/A_{600} and it was calculated by generating a concentration curve with a solution of purified elastase (EMD Millipore, Calbiochem #324676) dissolved in the same assay buffer.

The redox states of P. aeruginosa DsbA and LasB

P. aeruginosa strains were grown in LB overnight, washed with PBS buffer and diluted in 2 mL of M63 0.2% glucose media to an A_{600} of 0.01. Different concentrations of compound 12 dissolved in DMSO were added to a final concentration of 0.2% DMSO and incubated for 15 h at 37°C and shaken in a roller drum. Cells were then precipitated with TCA and alkylated with 12.5 mM of MalPEG-2 kDa (α-[3-(3-Maleimido-1-oxopropyl)amino]propyl-ω-methoxy, polyoxyethylene, NOF corporation) as described previously (Landeta *et al.,* 2015). For reduced controls, TCA-precipitated samples were treated with 100 mM Dithiothreitol (DTT, Sigma) for 30 min at room temperature. A 10 µg-aliquot of the total protein was diluted with non-reducing Laemmli loading buffer and subjected to SDS-PAGE (12% acrylamide, Biorad), semi-dry transfer and western blotting with 0.5 µg mL^{-1} of α-*Pa*DsbA antibody, which was raised using the whole protein without its signal sequence (*Pa*$DsbA_{Δ1-22}$, GenScript, USA). For elastase alkylation, we processed samples as described previously (Braun *et al.,* 2001). Briefly, *P. aeruginosa* strains were grown in LB overnight, the bacteria were washed with PBS buffer and diluted in 2 mL of M63 0.2% glucose media to an A_{600} of 0.01. Compound 12 was added to a final concentration of 50 µM in a final concentration of 0.2% DMSO and incubated for 22 h at 37°C and shaken in a roller drum. Cultures were centrifuged for 5 min at 13,000 rpm in a microcentrifuge. The recovered supernatant was used for alkylation with 20 mM NEM (N-Ethylmaleimide, Thermo Scientific). Proteins were precipitated as described above and a 7.5 µg-aliquot of the total protein was subjected to non-reducing SDS-PAGE (12% acrylamide, Biorad), semi-dry transfer and western blotting with α-*Pa*LasB antibody using a 1:6,000 dilution (Braun *et al.,* 2001).

Animals

For lung infection studies, female ICR mice weighing 22 ± 2 g were provided by BioLasco Taiwan (under Charles River Laboratories Licensee). Animals were acclimated for 3 days prior to use and were confirmed to be in good health. The space allocation for animals was 30 × 19 × 13 cm. All animals were maintained in a hygienic environment with controlled temperature (20-24°C), humidity (30-70%) and 12 h light/dark cycles. Free access to sterilized standard lab diet [MFG (Oriental Yeast Co., Ltd., Japan)] and autoclaved tap water were granted for the study duration. All aspects of this work, including housing, experimentation and disposal of animals were performed in general accordance with the Guide for the Care and Use of Laboratory Animals (National Academy Press, Washington, DC, 2011). The study was performed in AAALAC-accredited ABSL2 laboratory under the supervision of the veterinarians and the animal care and use protocol was approved by the IACUC at Eurofins Panlabs Taiwan.

For eye infection studies, the experimental protocols were approved by the Institutional Animal Care and Use Committee of the Harvard Medical Area, Office for Research Subject Protection and were consistent with the ARVO Animal Statement for the Use of Animals in Ophthalmic and Vision Research.

Lung infection studies with neutropenic mice (Third-party study by Eurofins)

Two pilot infection experiments (Supplementary Fig. 2 and Tables 2-1 to 2-6) were conducted with the parental wild-type PA14 strain to identify an optimal inoculum density. Groups of 6 female specific-pathogen-free ICR mice weighing 22 ± 2 g were used. Animals were immunosuppressed

by two intraperitoneal injections of cyclophosphamide, the first at 150 mg kg^{-1} four days before infection (day –4) and the second at 100 mg kg^{-1}, one day before infection (day –1). On day 0, animals were inoculated intranasally (0.02 mL/mouse) with target inoculation densities of 10^2, 10^3, 10^4, 10^5, 10^6 and 10^7 CFU per mouse of *P. aeruginosa* PA14 wild-type strain. Animals were first anesthetized with intravenous administration of etomidate-lipuro emulsion, 20 mg kg^{-1}, prior to inoculation. The actual inoculum densities were 2.02×10^2, 2.04×10^3, 1.86×10^4, 1.95×10^5, 1.85×10^6 and 1.80×10^7 CFU/mouse. Animals were sacrificed at 2 or at 26 h after inoculation with CO_2 asphyxiation and the lung tissues were harvested and weighted from each of the test animals. The removed lungs were homogenized in 1 mL of sterile PBS, pH 7.4 and then 10-fold serial dilutions were generated. Aliquots of the dilutions (100 µL) were separately plated onto MacConkey II agar plates. The bacterial counts (CFU g^{-1}) in lung tissues were calculated. 10^4-inoculum was selected for the main study to compare virulence between strains. To evaluate strain virulence, groups of 20 neutropenic mice were intranasally infected with a target density of 10^4 CFU/mouse of each strain. Bacterial counts were measured in lung tissue of 5 animals sacrificed at 2 h after infection and 15 animals sacrificed at 26 h after infection.

Eye infection studies in mice (Harvard Medical School)

Scratch-injured eyes of anesthetized C57BL/6 female mice ($N = 5$ per group; 6 weeks old) were challenged *in vivo* with the *P. aeruginosa* PA14 or mutants as described before (Preston *et al.,* 1995). Briefly, the infecting inoculum was delivered in a 5 µL volume with ~10^7 CFU/eye. The actual bacterial counts for experiment shown in Fig. 2B were WT: $1x10^7$, Δ*dsbB1B2*: $1.4x10^7$ and Δ*dsbA1A2*: $1.1x10^7$ CFU/eye. The actual bacterial counts for experiment shown in Fig. 2C were Δ*dsbB1B2*: $1x10^7$, Δ*dsbA1A2*: $1x10^7$, Δ*dsbB1B2*pJN105-*dsbB1*: $1.2x10^7$ and Δ*dsbA1A2*pJN105*dsbA1*: $1.6x10^7$ CFU/eye. The severity of corneal disease was scored by a masked observer on a scale of 0 to 4: 0, eye macroscopically identical with the uninfected contralateral control eye; 1, faint opacity partially covering the pupil; 2, dense opacity covering the pupil; 3, dense opacity covering the entire anterior segment; 4, perforation of the cornea, phthisis bulbi (shrinkage of the globe after inflammatory disease), or both. The disease severity scores observed at 48 h after infection were determined, the mice were euthanized by CO_2 and the extracellular and internalized Colony Forming Units (CFU) of *P. aeruginosa* were determined by serial dilution and plating. The excised corneas were placed in DMEM with 1% fetal bovine serum (FBS) and mixed with a Vortex mixer for 1 minute. The extracellular bacterial counts were determined from the solution obtained after vortexing. Each cornea was removed from the solution and placed in a solution of DMEM with 500 µg mL^{-1} gentamicin and 1% FBS and incubated for 1 h at 37°C, to kill any remaining extracellular bacteria. After exposure to gentamicin, the cornea was removed from the gentamicin solution and washed three times in 5 mL solution of DMEM 1% FBS. Next, the cornea was homogenized with 0.5% Triton X-100 in trypticase soy broth, serial dilutions were made in DMEM 1% FBS and bacteria were plated for enumeration of the intracellular or invading bacterial population.

VKOR knockdown in M. tuberculosis using CRISPRi-dCas9$_{Sth1}$

In order to silence VKOR expression, we used a dCas9$_{Sth1}$ system reported elsewhere (Rock *et al.,* 2017). The system uses a vector that expresses *dcas*9 under the control of a Tet promoter (TetR) and PAM sequences with different degrees of strength in silencing genes (Rock *et al.,* 2017). The ~20 bp *vkor* (Supplementary Fig. 6) targeting region was cloned into the sgRNA scaffold under the control of a constitutive promoter. All vectors were transformed into *M. tuberculosis* and selected for kanamycin resistance. Induction of *dcas9* with ATc caused poor growth of *M. tuberculosis* strains with strongest PAM sequences (Supplementary Fig. 6). Expression of VKOR was determined in the strains that yielded enough cell lysates and total protein (quantified by Pierce BCA kit, Thermo Scientific) to be analyzed by SDS-PAGE and western blotting using 2 µg mL^{-1} of α-*Mt*VKOR antibody (raised in rabbit using the PMRENRGSQERVGAR peptide as immunogen) and anti-*Ec*RpoA (4RA2; BioLegend, USA). *Mt*VKOR band intensity was estimated using ChemiDoc-XRS choosing wild-type as a reference band. JR1740 strain was selected due to its lower VKOR levels and partial growth.

M. tuberculosis H37Rv growth inhibition

A culture of *M. tuberculosis* was grown to stationary phase and diluted to A_{600} of 0.005. Compounds (in DMSO, final concentration 1%) were dissolved in 100 µL of 7H9 medium (±ATc) and subsequent serial two-fold dilutions were performed in 96-well plates. A bacterial inoculum of 100 µL was added to each well, yielding a final volume of 200 µL/well. Each compound was tested in triplicate and repeated with bacteria grown in Middlebrook 7H9 medium (Difco) supplemented with 0.2% glycerol, 0.05% Tween 80 (Sigma) and OADC (Becton Dickinson). The plates were sealed with breathable membranes and incubated in a shaker at 37°C. After seven days, 10 µL of Alamar Blue reagent (Biosource) was added to each well and the plates were incubated for 48 h at 37°C. The MIC was defined as the lowest drug concentration that prevented a color change from blue to pink.

Ethical statement

This study was carried out in strict accordance with the recommendations in the Guide for the Care and Use of Laboratory Animals (National Academy Press, Washington, DC, 2011) and in accordance with Institutional Animal Care and Use Committee of the Harvard Medical Area, Office for Research Subject Protection and were consistent with the ARVO Animal Statement for the Use of Animals in Ophthalmic and Vision Research. The protocol was approved by the Committee on the Ethics of Animal Experiments of Harvard Medical School.

Conflict of interest

Authors declare no conflict of interest.

Author contributions

C.L. and L.M. performed screening. C.L. performed *Pa* experiments. L.M. performed PDI experiments. N.Q.T. performed protein purification and *in vitro* experiments. Y.Z. and Z.T. performed mice experiments. C.L., S.W., J.R., R.A., M.T. and J.P. performed *Mtb* experiments. B.M.M., T.K. and D.B.1 provided tools for *Pa* experiments. C.L., L.M., B.M.M., E.J.R., S.L., G.P., D.B.2. and J.B. analyzed and discussed the data. C.L. and J.B. wrote the paper with input from all authors.

Acknowledgements

We thank the ICCB-Longwood screening facility for access to their compound libraries, equipment, screening supplies and to the staff including Richard Siu, Rachel Warden, Stewart Rudnicki and Jennifer Smith for equipment handling. We thank Lynn Miesel from Eurofins for helpful discussion in pneumonia model experiments as well as Su Chiang, Tom Dougherty, Ulrike Obst-Sander and David Mark for helpful advice and discussion throughout the entire project. We also thank Feras Hatahet for helpful advice in membrane protein purification and Jan Tommassen for kindly providing LasB antibody. This work was supported by US National Institute of General Medical Sciences grants GMO41883 (to J.B. and D.B.) and by an industry research agreement with F. Hoffmann-La Roche Ltd. and F. Hoffmann-La Roche Inc. (to J. B. and D.B.).

References

Amann, E., Ochs, B., and Abel, K. (1988) Tightly regulated tuc promoter vectors useful for the expression of unfused and fused proteins in *Escherichia coli* (Recombinant DNA; plasmids; trc promoter; lacZ-coded repressor; lac operator; cat gene; eukaryotic protein overproduction; human coa. *Gene*, **69**, 301–315.

Arts, I.S., Ball, G., Leverrier, P., Garvis, S., Nicolaes, V., Vertommen, D., *et al*. (2013) Dissecting the machinery that introduces disulfide bonds in *Pseudomonas aeruginosa*. *mBio*, **4**, 1–11.

Awasthi, D., and Freundlich, J.S. (2017) Antimycobacterial metabolism: illuminating *Mycobacterium tuberculosis* biology and drug discovery. *Trends in Microbiology*, **25**, 756–767.

Bardwell, J.C., Lee, J.O., Jander, G., Martin, N., Belin, D., and Beckwith, J. (1993) A pathway for disulfide bond formation in vivo. *Proceedings of the National Academy of Sciences*, **90**, 1038–1042.

Bardwell, J.C.A., McGovern, K., and Beckwith, J. (1991) Identification of a protein required for disulfide bond formation in vivo. *Cell*, **67**, 581–589.

Braun, P., Ockhuijsen, C., Eppens, E., Koster, M., Bitter, W., and Tommassen, J. (2001) Maturation of *Pseudomonas aeruginosa* elastase: formation of the disulfide bonds. *Journal of Biological Chemistry*, **276**, 26030–26035.

Cathcart, G.R., Gilmore, B.F., Greer, B., Harriott, P., and Walker, B. (2009) Inhibitor profiling of the *Pseudomonas aeruginosa* virulence factor LasB using N-alpha mercaptoamide template-based inhibitors. *Bioorganic & Medicinal Chemistry Letters*, **19**, 6230–6232.

Dutton, R.J., Boyd, D., Berkmen, M., and Beckwith, J. (2008) Bacterial species exhibit diversity in their mechanisms and capacity for protein disulfide bond formation. *Proceedings of the National Academy of Sciences*, **105**, 11933–11938.

Dutton, R.J., Wayman, A., Wei, J.-R., Rubin, E.J., Beckwith, J., and Boyd, D. (2010) Inhibition of bacterial disulfide bond formation by the anticoagulant warfarin. *Proceedings of the National Academy of Sciences*, **107**, 297–301.

Folkesson, A., Jelsbak, L., Yang, L., Johansen, H.K., Ciofu, O., Hoiby, N., *et al*. (2012) Adaptation of *Pseudomonas aeruginosa* to the cystic fibrosis airway: an evolutionary perspective. *Nature Reviews Microbiology*, **10**, 841–851.

Fujitani, S., Sun, H.Y., Yu, V.L., and Weingarten, J.A. (2011) Pneumonia due to *Pseudomonas aeruginosa*: part I: epidemiology, clinical diagnosis, and source. *Chest*, **139**, 909–919.

Global Tuberculosis Report (2017). Geneva: World Health Organization; 2017.

Ha, U., Wang, Y., and Jin, S. (2003) DsbA of *Pseudomonas aeruginosa* is essential for multiple virulence factors. *Infection and Immunity*, **71**, 1590–1595.

Harvey, H., Habash, M., Aidoo, F., and Burrows, L.L. (2009) Single-residue changes in the C-terminal disulfide-bonded loop of the *Pseudomonas aeruginosa* type IV pilin influence pilus assembly and twitching motility. *Journal of Bacteriology*, **191**, 6513–6524.

Hatahet, F., Blazyk, J.L., Martineau, E., Mandela, E., Zhao, Y., Campbell, R.E., *et al*. (2015) Altered *Escherichia coli* membrane protein assembly machinery allows proper membrane assembly of eukaryotic protein vitamin K epoxide reductase. *Proceedings of the National Academy of Sciences*, **112**, 15184–15189.

Heras, B., Totsika, M., Jarrott, R., Shouldice, S.R., Gunčar, G., Achard, M.E.S., *et al*. (2010) Structural and functional characterization of three DsbA paralogues from *Salmonella enterica* serovar typhimurium. *Journal of Biological Chemistry*, **285**, 18423–18432.

Horton, R. (1993) In vitro recombination and mutagenesis of DNA. *Methods in Molecular Biology*, **15**, 251–261.

Inaba, K., Murakami, S., Nakagawa, A., Iida, H., Kinjo, M., Ito, K., and Suzuki, M. (2009) Dynamic nature of disulphide bond formation catalysts revealed by crystal structures of DsbB. *The EMBO Journal*, **28**, 779–791.

Kadokura, H., and Beckwith, J. (2002) Four cysteines of the membrane protein DsbB act in concert to oxidize its substrate DsbA. *The EMBO Journal*, **21**, 2354–2363.

Ke, N., Landeta, C., Wang, X., Boyd, D., Eser, M., and Beckwith, J. (2018) Identification of the thioredoxin partner of VKOR in mycobacterial disulfide bond formation. *Journal of Bacteriology*, **200**, e00137–18.

Kim, S.H., Park, S.Y., Heo, Y.J., and Cho, Y.H. (2008) Drosophila melanogaster-based screening for multihost virulence factors of *Pseudomonas aeruginosa* PA14 and

identification of a virulence-attenuating factor, HudA. *Infection and Immunity*, **76**, 4152–4162.
Kurosu, M., and Begari, E. (2010) Vitamin K2 in electron transport system: are enzymes involved in vitamin K2 biosynthesis promising drug targets?*Molecules*, **15**, 1531–1553.
Landeta, C., Blazyk, J.L., Hatahet, F., Meehan, B.M., Eser, M., Myrick, A., *et al*. (2015) Compounds targeting disulfide bond forming enzyme DsbB of Gram-negative bacteria. *Nature Chemical Biology*, **11**, 292–298.
Landeta, C., Boyd, D., and Beckwith, J. (2018) Disulfide bond formation in prokaryotes. *Nature Microbiology*, **3**, 270–280.
Landeta, C., Meehan, B.M., McPartland, L., Ingendahl, L., Hatahet, F., Tran, N.Q., *et al*. (2017) Inhibition of virulence-promoting disulfide bond formation enzyme DsbB is blocked by mutating residues in two distinct regions. *Journal of Biological Chemistry*, **292**, 6529–6541.
Li, W., Schulman, S., Dutton, R.J., Boyd, D., Beckwith, J., and Rapoport, T.A. (2010) Structure of a bacterial homologue of vitamin K epoxide reductase. *Nature*, **463**, 507–512.
Lin, D., Kim, B., and Slauch, J.M. (2009) DsbL and DsbI contribute to periplasmic disulfide bond formation in *Salmonella enterica* serovar Typhimurium. *Microbiology*, **155**, 4014–4024.
Lyczak, J.B., Cannon, C.L., and Pier, G.B. (2000) Establishment of *Pseudomonas aeruginosa* infection: lessons from a versatile opportunist. *Microbes and Infection*, **2**, 1051–1060.
Madshus, I.H., and Collier, R.J. (1989) Effects of eliminating a disulfide bridge within domain II of *Pseudomonas aeruginosa* exotoxin A. *Infection and Immunity*, **57**, 1873–1878.
Maschmeyer, G., and Braveny, I. (2000) Review of the incidence and prognosis of *Pseudomonas aeruginosa* infections in cancer patients in the 1990s. *European Journal of Clinical Microbiology & Infectious Diseases*, **19**, 915–925.
Meehan, B.M., Landeta, C., Boyd, D., and Beckwith, J. (2017a) The disulfide bond formation pathway is essential for anaerobic growth of *Escherichia coli*. *Journal of Bacteriology*, **199**, e00120–17.
Meehan, B.M., Landeta, C., Boyd, D., and Beckwith, J. (2017b) The essential cell division protein FtsN contains a critical disulfide bond in a non-essential domain. *Molecular Microbiology*, **103**, 413–422.
Mizgerd, J., and Skerrett, S. (2008) Animal models of human pneumonia. *American Journal of Physiology-Lung Cellular and Molecular Physiology*, **294**, L387–L398.
Newman, J.R., and Fuqua, C. (1999) Broad-host-range expression vectors that carry the L-arabinose-inducible *Escherichia coli* araBAD promoter and the araC regulator. *Gene*, **227**, 197–203.
Page, M.G., and Heim, J. (2009) Prospects for the next anti-Pseudomonas drug. *Current Opinion in Pharmacology*, **9**, 558–565.
Potashman, M.H., and Duggan, M.E. (2009) Covalent modifiers: an orthogonal approach to drug design. *Journal of Medicinal Chemistry*, **52**(5), 1231–1246.
Preston, M.J., Fleiszig, S.M., Zaidi, T.S., Goldberg, J.B., Shortridge, V.D., Vasil, M.L., *et al*. (1995) Rapid and sensitive method for evaluating *Pseudomonas aeruginosa* virulence factors during corneal infections in mice. *Infection and Immunity*, **63**, 3497–3501.
Regeimbal, J., Gleiter, S., Trumpower, B.L., Yu, C.A., Diwakar, M., Ballou, D.P., *et al*. (2003) Disulfide bond formation involves a quinhydrone-type charge-transfer complex. *Proceedings of the National Academy of Sciences*, **100**, 13779–13784.
Rice, L.B. (2010) Progress and challenges in implementing the research on ESKAPE pathogens. *Infection Control & Hospital Epidemiology*, **31**, S7–S10.
Rock, J.M., Hopkins, F.F., Chavez, A., Diallo, M., Chase, M.R., Gerrick, E.R., *et al*. (2017) Programmable transcriptional repression in mycobacteria using an orthogonal CRISPR interference platform. *Nature Microbiology*, **2**, 1–9.
Rust, L., Messing, C.R., and Iglewski, B.H. (1994) Elastase assays. *Methods in Enzymology*, **235**, 554–562.
Sassetti, C.M., and Rubin, E.J. (2003) Genetic requirements for mycobacterial survival during infection. *Proceedings of the National Academy of Sciences*, **100**, 12989–12994.
Tian, H., Boyd, D., and Beckwith, J. (2000) A mutant hunt for defects in membrane protein assembly yields mutations affecting the bacterial signal recognition particle and Sec machinery. *Proceedings of the National Academy of Sciences*, **97**, 4730–4735.
Urban, A., Leipelt, M., Eggert, T., and Jaeger, K.E. (2001) DsbA and DsbC affect extracellular enzyme formation in *Pseudomonas aeruginosa*. *Journal of Bacteriology*, **183**, 587–596.
Wang, X., Dutton, R.J., Beckwith, J., and Boyd, D. (2011) Membrane topology and mutational analysis of *Mycobacterium tuberculosis* VKOR, a protein involved in disulfide bond formation and a homologue of human vitamin K epoxide reductase. *Antioxid Redox Signal*, **14**, 1413–1420.
Weiss, D.S., Chen, J.C., Ghigo, J.M., Boyd, D., and Beckwith, J. (1999) Localization of FtsI (PBP3) to the septal ring requires its membrane anchor, the Z ring, FtsA, FtsQ, and FtsL. *Journal of Bacteriology*, **181**, 508–520.
Zhao, M., Lepak, A.J., and Andes, D.R. (2016) Bioorganic & medicinal chemistry animal models in the pharmacokinetic/pharmacodynamic evaluation of antimicrobial agents. *Bioorganic & Medicinal Chemistry*, **24**, 6390–6400.

Supporting Information

Additional supporting information may be found online in the Supporting Information section at the end of the article